GeoExpert ag

swiss*nuclear*: PEGASOS Refinement Project:
SP2 – Ground Motion Characterization

Contract no. PMT-VT-1032

Seismic Shear Wave Velocity Determination and Hybrid Seismic Survey at the SED-Station BALST (Mümliswil, SO)

Date of Field Data Acquisition 6th May 2009

Report

Client

swiss*nuclear*
Project PRP
Frohburgstrasse 17
4601 Olten

Contractor

GeoExpert ag
Seismic Prospecting
Ifangstrasse 12b
P.O. Box 451
8603 Schwerzenbach

8603 Schwerzenbach, 7th July 2009

INDEX

1 INTRODUCTION....3
1.1 Survey objectives....3
1.2 The choice of the appropriate surveying methods....3
2 FIELD DATA ACQUISITION PARTICULARS....4
2.1 Time Schedule....4
2.2 Summary of Data Acquisition Parameters....4
2.3 Composition of Seismic Field Crew....4
2.4 Location....5
2.5 Recording Conditions and Line Setup....5
3 SEISMIC DATA PROCESSING AND IMAGING OF THE RESULTS....7
3.1 General Remarks....7
3.2 Shear Wave Refraction Tomography....7
3.2.1 Reformatting and field geometry assignment....7
3.2.2 First break time picking....7
3.2.3 Analytical Determination of Refraction Velocities....8
3.2.4 Tomographic inversion of the velocity gradient field by iterative modeling....9
3.3 MASW Processing....12
3.3.1 Reformatting and field geometry assignment....12
3.3.2 Calculating the dispersion image (overtone)....12
3.3.3 Analysis of the dispersion image....12
3.3.4 Inversion of dispersion curves resulting in a 1D shear wave velocity distribution....15
3.3.5 Gridding and plotting of 2D vs-velocity field....18
3.3.6 Calculation of the average shear wave velocity....19
3.3.7 Calculation of the shear wave velocity scalars vs,5, vs,10, ...21
3.4 Hybrid Seismic Data Processing....22
3.4.1 p-wave Reflection Seismic Processing Sequence....22
3.4.2 The presentation of reflection seismic data....22
3.4.3 p-wave refraction tomography processing....25
3.4.4 Representation of the hybrid seismic section....29
4 DISCUSSION OF THE RESULTS 31
4.1 Summary and Validation of the Results....31
4.2 Validation of the methods and their results....31
4.3 Error Estimates....32
4.4 The Geophysical Interpretation....33
5 SUMMARY AND CONCLUSIONS....35

1 INTRODUCTION

1.1 Survey objectives

The seismic survey's main task is to provide information about the distribution function of the shear wave velocities in the depth interval of the uppermost 30 m along a 100 m long seismic profile.

Additionally, the following objectives are to be met:

- the mapping of the topography of the rock face, i.e. the thickness of the Quaternary deposits;
- the determination of the thickness of the weathered zone and its degree of decompaction at the bedrock surface;
- a general view of geological structures.

1.2 The choice of the appropriate surveying methods

Several methods are available for deriving the s-wave velocity distribution in the subsurface at any given position:

- in-situ measurement by down-hole or crosshole seismic surveying;
- shear-wave refraction tomography profiling;
- dispersion analysis of surface waves (MASW; **M**ultiple channel **A**nalysis of **S**urface **W**aves)

The surveys are to be carried out at, or as close as possible near some 20 SED earth quake monitoring stations in Switzerland. Ideally, the surveys are to be conducted on two orthogonal profiles in order to derive at their point of intersection a robust 1D s-wave velocity distribution function by correlation. To this end, the methods of MASW and shear-wave refraction tomography profiling are to be combined.

The results are to include the following fundamental parameters $v_{s,5}$, $v_{s,10}$, $v_{s,20}$, $v_{s,30}$, $v_{s,40}$, $v_{s,50}$, $v_{s,100}$ are to be calculated, also an error estimation of all values.

The data acquired for the MASW method are to be subjected to complementary **p-wave hybrid seismic data processing** in order to image the geological structures.

2 FIELD DATA ACQUISITION PARTICULARS

2.1 Time Schedule

Date	*Time*	*Activities / remarks*
06.05.2009	0645 - 0800	arrival at site
	0815 - 0830	site investigation
	0830 - 1130	lay-out of spread profile 1 (p-wave and s-wave)
	1130 - 1215	data acquisition of spread profile 1 (p-wave)
	1245 - 1330	data acquisition of spread profile 1 (s-wave)
	1330 - 1400	lay-out of spread profile 2 (p-wave and s-wave)
	1400 - 1440	data acquisition of spread profile 2 (p-wave)
	1440 - 1535	data acquisition of spread profile 2 (s-wave)
	1535 - 1630	removal of the seismic measuring system
	1630 - 1800	leaving from site

2.2 Summary of Data Acquisition Parameters

Compressional Wave Data Acquisition

# of active channels	96
geophone type	4.5 Hz natural frequency, vertical velocimeter
receiver station spacing	1.0 m
# of geophones/station	1
source point spacing	2.0 m to 3.0 m
source type	vertical hammer (8 kg) striking on a horizontal metal plate
sampling rate	500 µs
recording time	2048 ms
field filters	0.5 Hz LC, anti-alias
# of field records	49 (line 09SN_08BALST-P1) and 46 (line 09SN_08BALST-P2)

Shear Wave Data Acquisition

# of active channels	48
geophone type	10 Hz natural frequency, horizontal velocimeter
receiver station spacing	2.0 m
# of geophones/station	1
source point spacing	4.0 m to 6.0 m
source type	horizontal hammer (8 kg) striking horizontally at a metal-plated wooden beam anchored to the ground by means of 20 cm long spikes
sampling rate	500 µs
recording time	512 ms
field filters	2 Hz LC, anti-alias
# of field records	48 (line 09SN_03BALST-S1) and 50 (line 09SN_03BALST-S2)

2.3 Composition of Seismic Field Crew

Personnel

Jochen Fiseli	Dipl.-Geologist, University of Freiburg i. Br., party chief
Dieter Martin	Dipl.-Geologist, University of Freiburg i. Br., party chief
Kieron Lynch	assistant, spread lay-out and activation of seismic source
Fabian Isler	assistant, spread lay-out and activation of seismic source

Equipment

96	vertical geophones 4.5 Hz
48	horizontal geophones 12 Hz
6	seismic cables
1	seismic acquisition system Summit Compact, 96 channels
1	laptop computer for data acquisition
3	walkie-talkies
1	hammer 8 kg
1	steel plate
1	metal-plated wooden beam
1	van (FIAT Ducato 4x4)

2.4 Location

The seismic monitoring station BALST (Mümliswil, SO) is situated on the top of a karstified Jurassic (Malm) sediment plateau, encircled by elder (Dogger) and younger (USM) sediments, in the Jura ridge, Switzerland, canton of Solothurn.

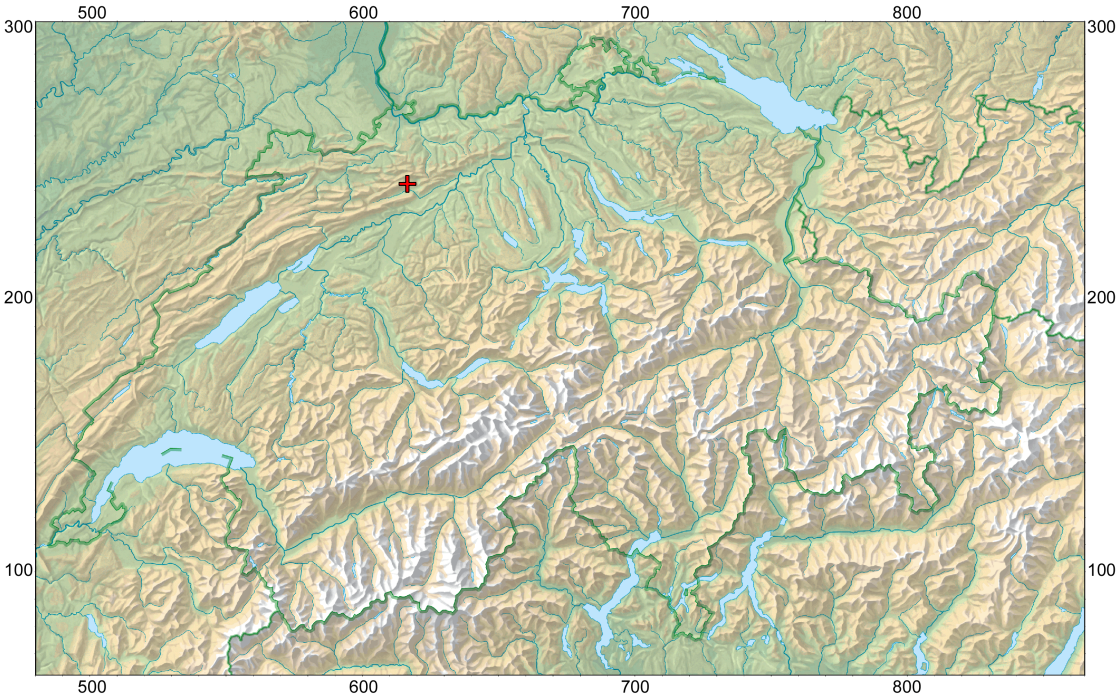

Fig. 2.2: The red cross marked seismic monitoring station BALS (Balsthal SO) is located in Solothurns Jurassic sediments (Malm). (map: geodata @ swisstopo).

2.5 Recording Conditions and Line Setup

Pleasant temperatures prevailed throughout the field data recording period.

In general, the data quality obtained at BALST is to be rated as good. Data from profile 09SN_03BALST contents noise from unidentified sources.

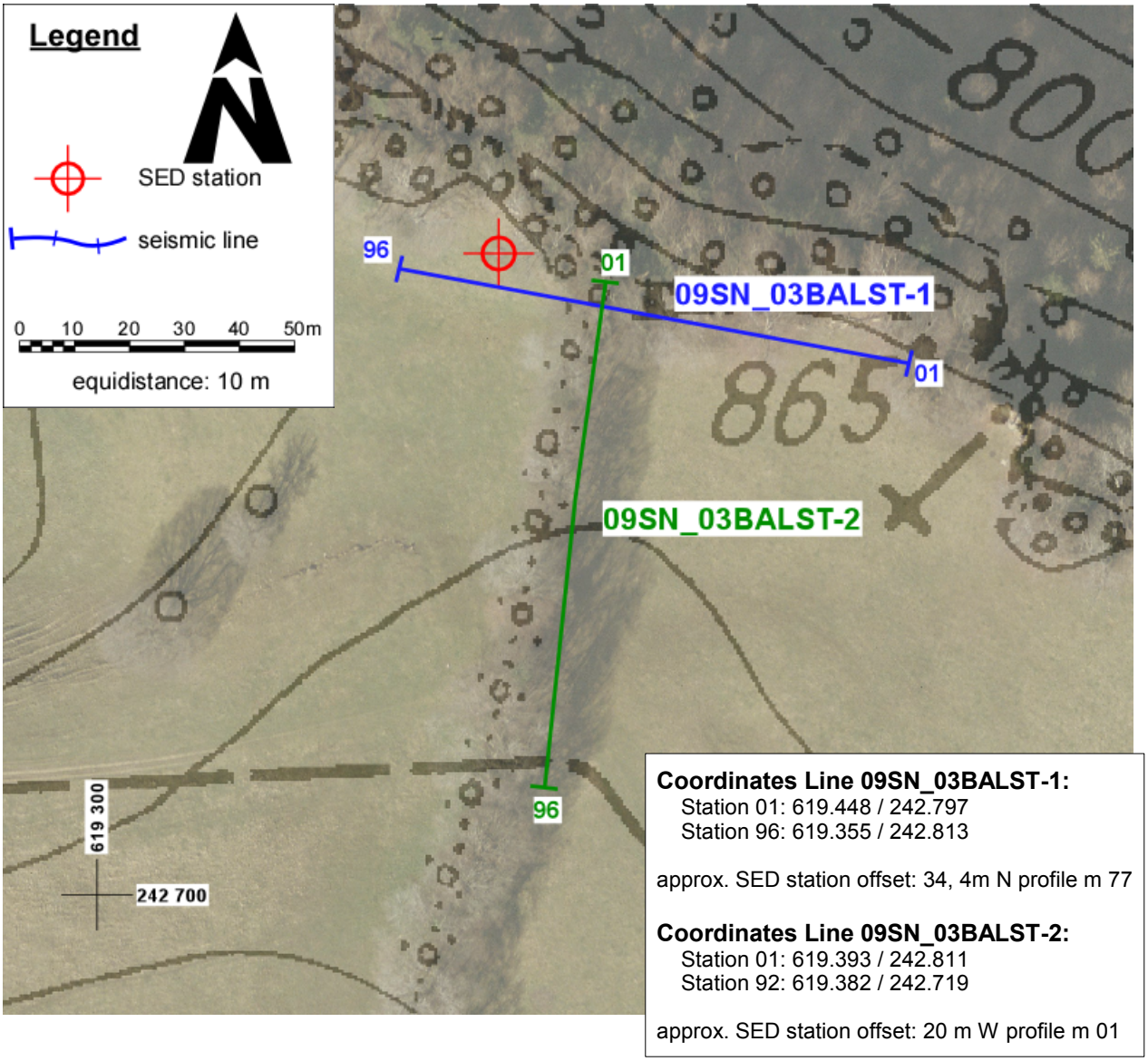

Fig. 2.3: Situation map with the trace of seismic profile 09SN_03BALST-1 and -2. (background map: © Amt für Geoinformation Kt. Solothurn, www.agi.so.ch)

3 SEISMIC DATA PROCESSING AND IMAGING OF THE RESULTS

3.1 General Remarks

- For the shear and compressional wave refraction seismic evaluation the package **RAYFRACT** by Intelligent Resources Ltd., Vancouver CAN, was used. The system features the technique of diving wave tomography (www.rayfract.com).
- The system **SPW** (**S**eismic **P**rocessing **W**orkshop) of Parallel Geoscience Corporation, Austin US-TX, was used for reflection seismic data processing (www.parallelgeo.com).
- Data processing of surface waves (MASW processing) was conducted with the software package **SurfSeis** V2.0 of Kansas Geological Survey in Lawrence US-KS.

A detailed description of the various surveying methods will be included in the general summary report.

3.2 Shear Wave Refraction Tomography

3.2.1 Reformatting and field geometry assignment

After reformatting the field data into the Rayfract format the field geometry is applied.

3.2.2 First break time picking

At each shot position, two seismic records were acquired in both activation directions. These two records are displayed superimposed with different colors on each other in Fig 3.2a together with the manually determined first arrival time picks.

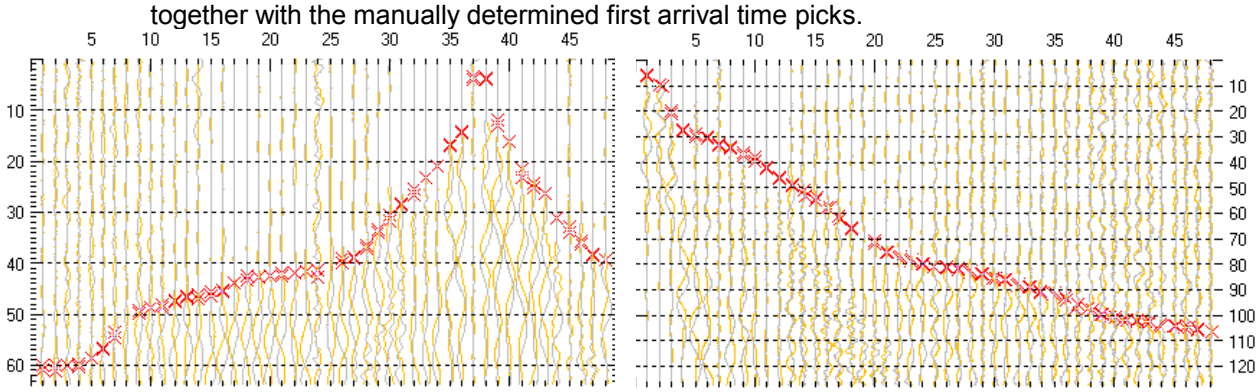

*Fig. 3.2a: High quality dual field record of line 09SN_03BALST-S1 (left) and -S2 (right).showing at each station the s-wave traces with opposing polarities in different colors. The manually picked s-wave refraction arrivals at each station are marked with an **x**. The station spacing is 2 m, profile station number 00 = profile meter 0; profile station number 48 = profile meter 96.*

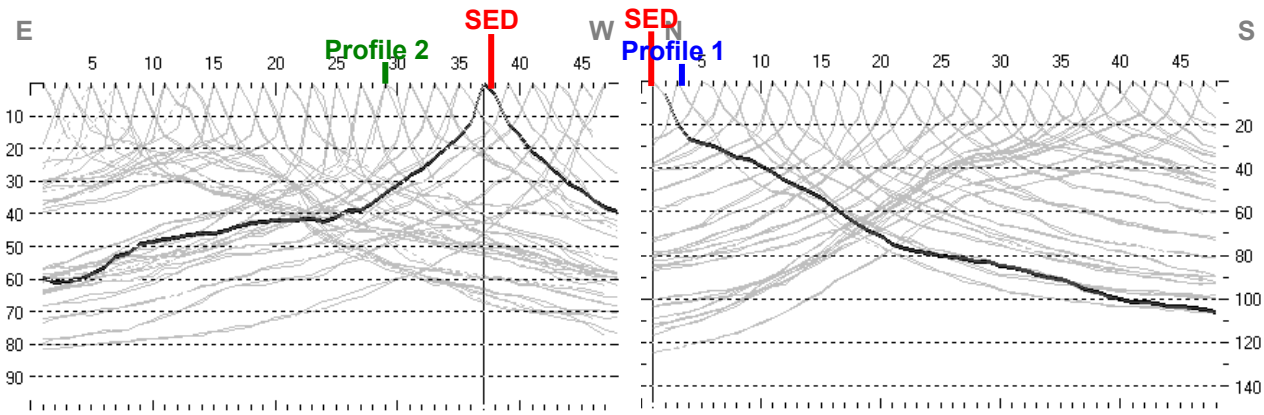

Fig. 3.2b: Curves of s-wave first break time picks of line 09SN_03BALST-S1 (left) and -S2 (right).

3.2.3 Analytical Determination of Refraction Velocities

An initial 1D-velocity function (averaged 1D velocity-depth profiles derived by the Delta-t-V method, see Tab. 3.2a) is determined in the 3-dimensional time-offset-CMP-domain of all first break arrival time curves in the 3-dimensional time-offset-CMP-domain (see. Fig. 3.2c).

Depth [m]	Vs [m/s]
0.0	213
0.5	305
0.9	348
1.4	440
2.1	586
3.0	776
4.4	1054
6.2	1227
8.9	1321
12.4	1605
17.2	2135
24.0	2812
33.4	3803
46.2	4238

Depth [m]	Vs [m/s]
0.0	198
0.5	281
0.9	308
1.4	360
2.1	475
3.4	715
4.8	1002
7.0	1447
10.0	1290
14.3	970
20.2	1129
28.4	1639
40.0	2397
56.0	3153

Tab. 3.2a: Initial 1D s-wave velocity function derived from real data of line 09SN_03BALST-S1 (mean values between profile meters 10 and 60) and of line 09SN_03BALST-S2 (mean values between profile meters 60 and 96).

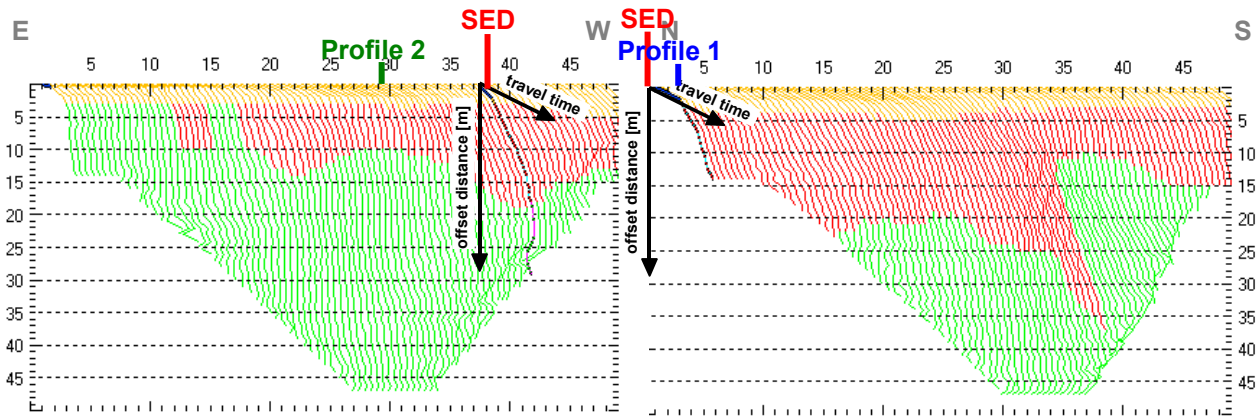

Fig. 3.2c: 3-dimensional distance-travel time diagrams of line 09SN_03BALST-S1 (left) and -S2 (right) at the mid-points between source points and receiver stations are instrumental when using the analytical CMP derivation of the initial velocity field.
The horizontal axes are the along the CMP positions and the travel time respectively, the vertical axis denotes the offset distance between source and receiver positions. The colors represent different velocity layers. The station spacing is 2 m, profile station number 00 = profile meter 0; profile station number 48 = profile meter 96. The colors represent different velocity layers.

3.2.4 Tomographic inversion of the velocity gradient field by iterative modeling

The velocity field is iteratively refined by the subsequent Wavepath Eikonal Traveltime (WET) tomographic inversion process. The inversion results are portrayed in Fig. 3.2d as a gridded velocity contour section and in Fig. 3.2e as a ray path density section.

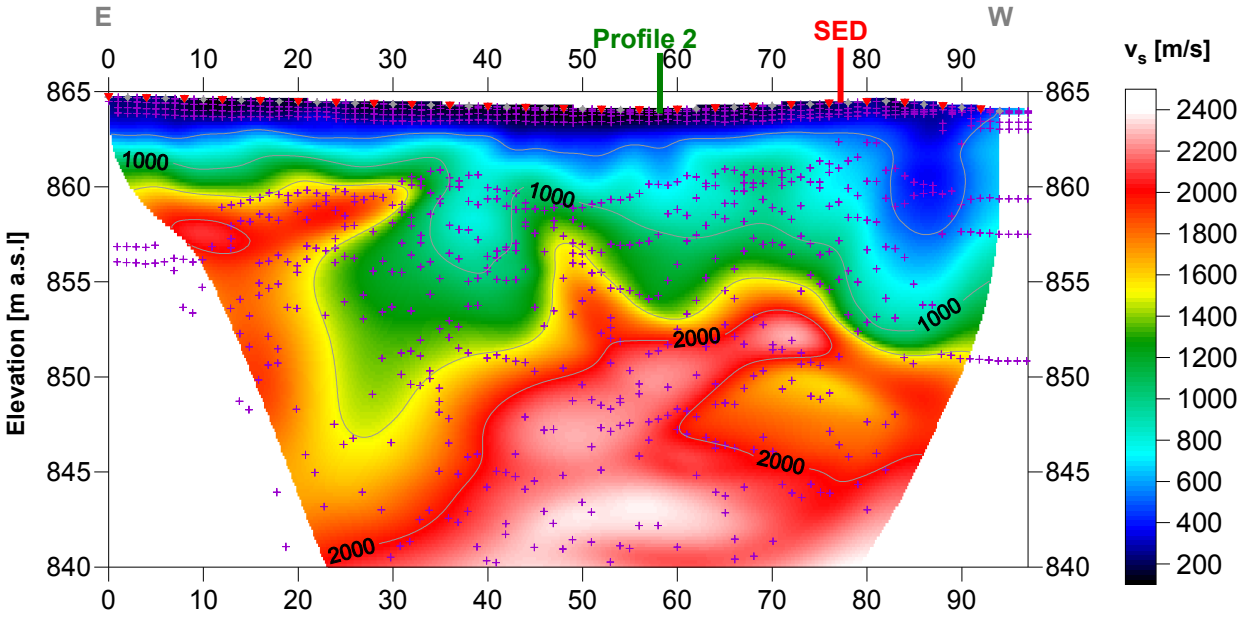

Fig. 3.2d: Shear wave velocity field of the line 09SN_03BALST-S1. Red/white colors denote solid rock, blue/black colors point to unconsolidated sediments and soil.
Vertical axis: elevation [m a.s.l]; horizontal axis: profile meter; color encoded scale: v_s [m/s]; vertical exaggeration: 2:1; gray diamonds: receiver positions; red triangles: source positions; magenta crosses: positions of determined velocity values. The station spacing is 2 m, profile meter 0 = profile station number 00, profile meter 96 = profile station number 48.

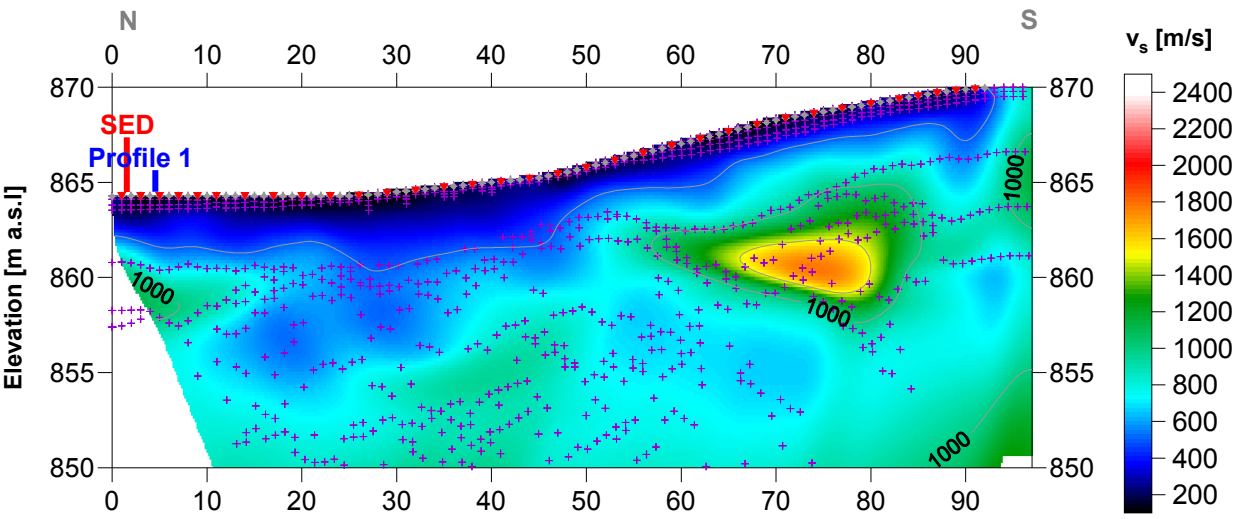

Fig. 3.2e: Shear wave velocity field of the line 09SN_03BALST-S2. Red/white colors denote solid rock, blue/black colors point to unconsolidated sediments and soil.
Vertical axis: elevation [m a.s.l]; horizontal axis: profile meter; color encoded scale: v_s [m/s]; vertical exaggeration: 2:1; gray diamonds: receiver positions; red triangles: source positions; magenta crosses: positions of determined velocity values. The station spacing is 2 m, profile meter 0 = profile station number 00, profile meter 96 = profile station number 48.

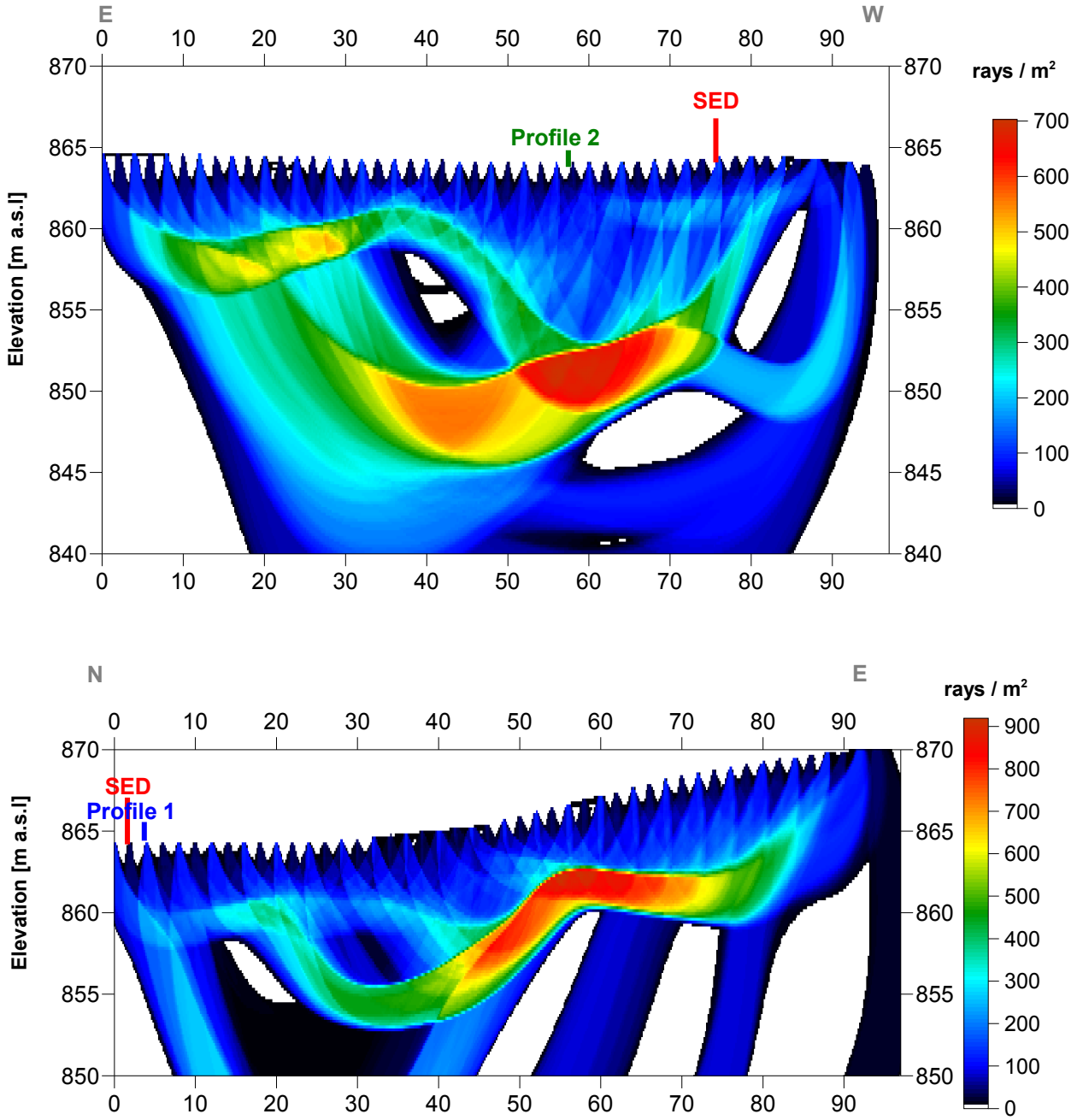

Fig. 3.2f: Shear wave ray path density along the seismic line 09SN_03BALST-S1 (top) and -S2 (bottom). Red/white colors indicate high velocity contrasts (usually at the bedrock surface), blue/black colors denote low coverage areas. Vertical axis: elevation [m a.s.l]; horizontal axis: profile meter; color encoded scale: ray paths per m²; vertical exaggeration: 2:1. The station spacing is 2 m, profile meter 0 = profile station 00, profile meter 96 = profile station 48.

Depth [m]	Vs [m/s]
0.0	155
2.0	610
3.9	1138
5.9	1336
7.8	1244
9.8	1313
11.7	1428
13.7	1614
15.6	1780
17.6	1843
19.5	1895
21.5	2037
23.4	2178
25.4	2323
27.3	2365
29.3	2236
31.2	2462
33.2	2588

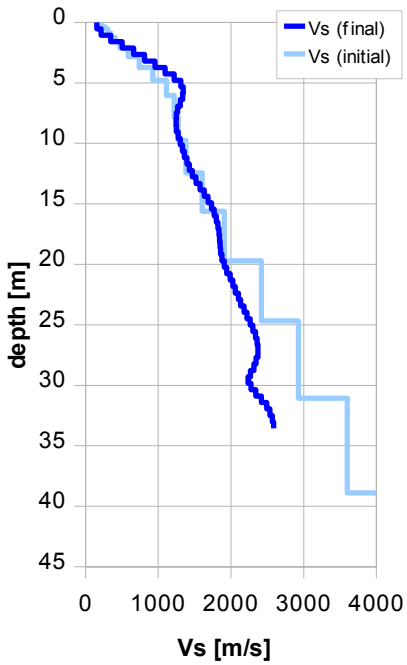

Tab. 3.2b: Final 1D s-wave velocity model derived from real data of line 09SN_03BALST-S1 (horizontal average of all values) for the profile segment (between profile meters 10 and 60) with a geological setting resembling the one at the SED station. The calculated values of the initial 1D s-wave velocity model are given in Tab. 3.2a.

Depth [m]	Vs [m/s]
0.0	245
2.1	600
4.3	877
6.4	1221
8.6	1146
10.7	817
12.7	734
14.8	774
17.0	867
19.1	965
21.2	1023
23.4	1066
25.3	1115
27.5	1161
29.6	1313
31.8	1428

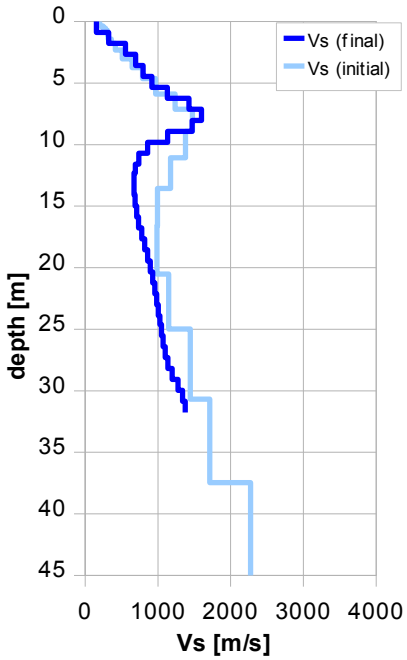

Tab. 3.2c: Final 1D s-wave velocity model derived from real data of line 09SN_03BALST-S2 (horizontal average of all values) for the profile segment (between profile meters 60 and 96) with a geological setting resembling the one at the SED station. The calculated values of the initial 1D s-wave velocity model are given in Tab. 3.2a.

3.3 MASW Processing

3.3.1 Reformatting and field geometry assignment

The data preparation steps for the dispersion analysis include

- the assignment of the field acquisition geometry
- the selection of suitable offset ranges (=arrays) between 10 m and 50 m for dispersion, and the splitting of the field records in forward and reverse shooting direction data sets
- the reformatting of the data into the specific KGS format

X - - ... - - o-o-o-...-o-o-o (forward shooting or so-called PLUS direction)
respectively
o-o-o-...-o-o-o - - ... - - X (reverse shooting or so-called MINUS direction).

where **X** = shot position
o = receiver station
- = 1.0 m offset

The active array used at SED-station BALST are the receiver station in the shot offset range between 10 and 50 m.

3.3.2 Calculating the dispersion image (overtone)

The result of dispersion analysis is the color encoded acoustic energy distribution in the phase velocity - frequency plane (see Fig. 3.3a and b).

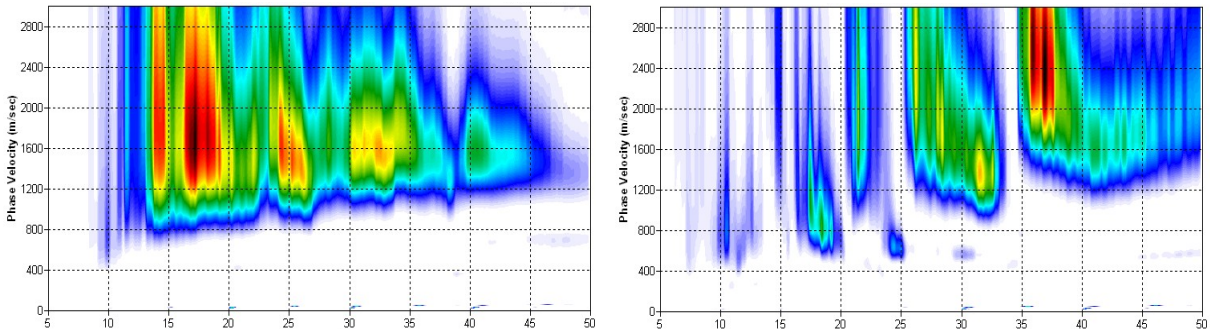

Fig. 3.3a: Dispersion image of fair to high quality data (left) as found on 70 % and of deficient quality data (right) representing about 30 % of the MASW dataset of site BALST. Horizontal axis: frequency from 5 to 50 Hz; vertical axis: phase velocity from 0 to 2000 m/s; color code: colors from white (no energy) to blue - green - yellow - red - black point to increasing energy amplitude values.

3.3.3 Analysis of the dispersion image

In the dispersion graphs as calculated in section 3.3.2 above, the curves joining the amplitude peaks of the fundamental modes are determined either by subjective inspection or in a semi-automated manner. On datasets with poorly defined amplitude peaks or with a highly irregular alignment of the peaks, the danger of obtaining improbable or wrong results is real and can only be mitigated by the processing experience and the a-priori knowledge of the geological setting by the geophysicist responsible for the data evaluation.

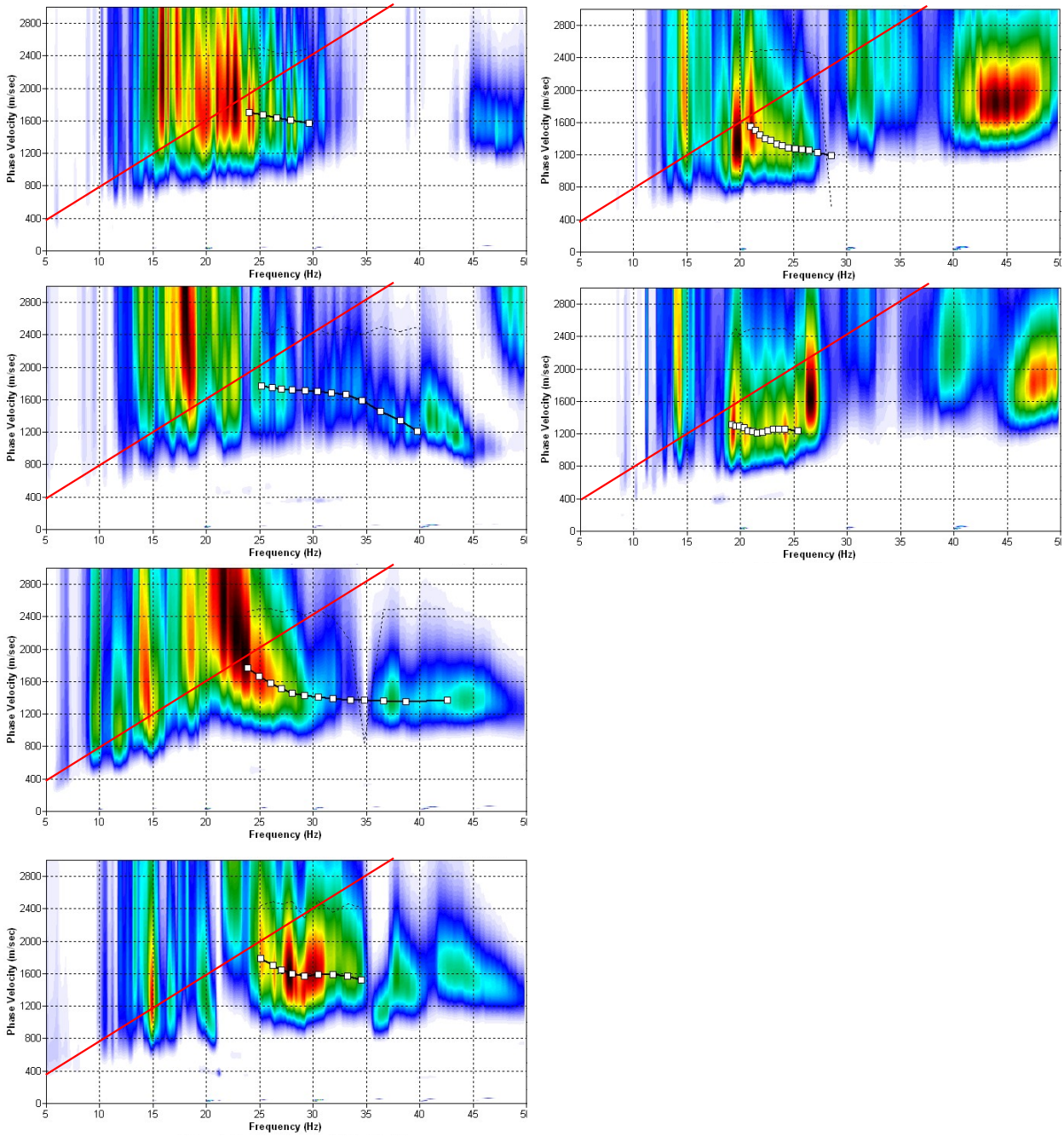

Fig. 3.3b: The manually picked dispersion images used for the derivation of the shear wave velocity section on line 09SN_03BALST-M1. The dispersion curves (squares) are determined by linking the peaks of high energy. Note that 'higher modes' may at times produce higher energy peaks than the fundamental mode required for the analysis.
dotted fine line: signal-noise ratio for the designated f-v_{ph} – value.
red line: high resolution beam-forming curve for v_{max}.
1st row: left: station 21 @ PLUS direction; right: station 24 @ MINUS direction
2nd row: left: station 33 @ PLUS direction; right: station 27 @ MINUS direction
3rd row: left: station 39 @ PLUS direction; right: not available due to bad quality
4th row: left: station 46 @ PLUS direction; right: not available due to bad quality

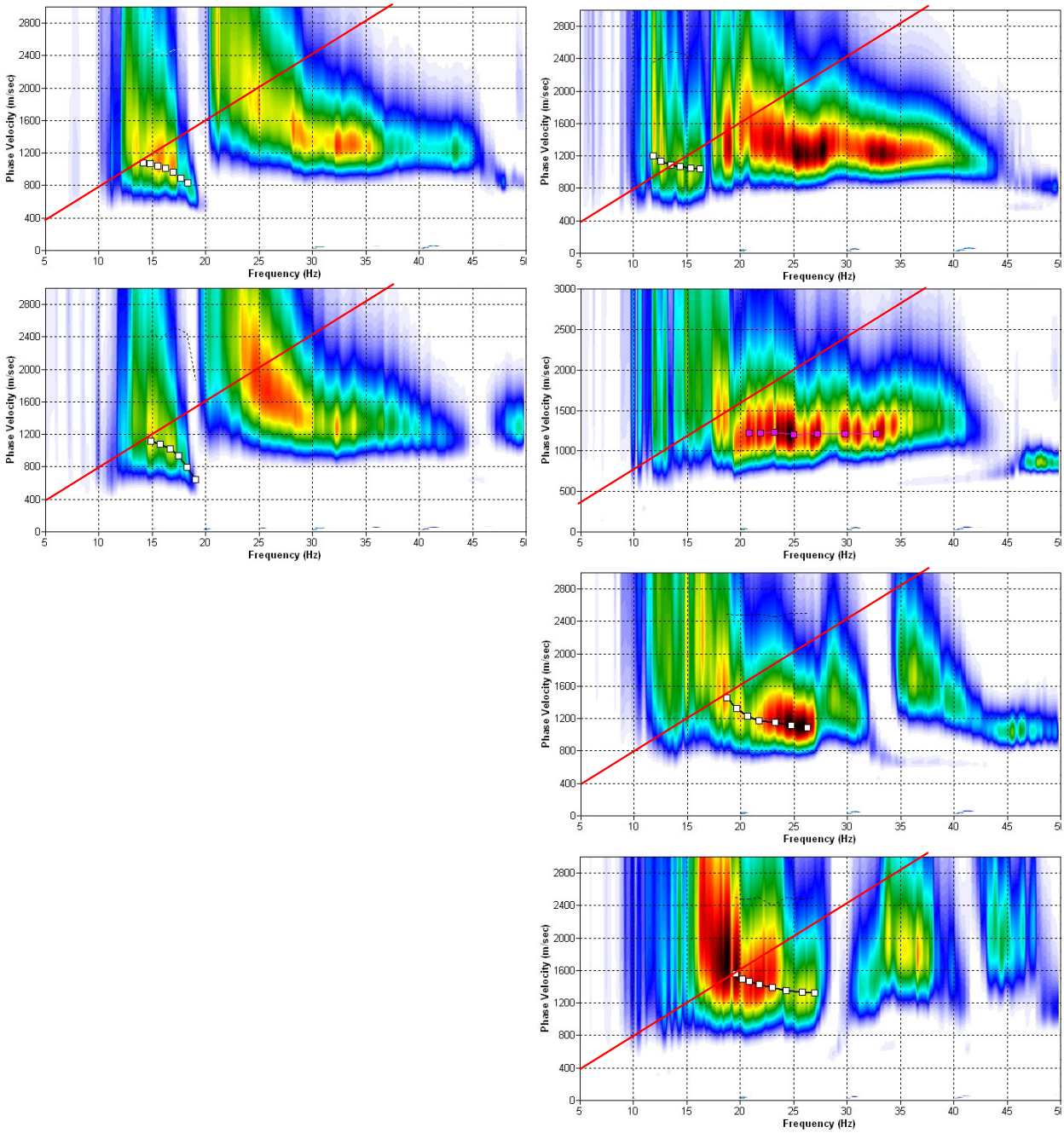

Fig. 3.3c: The manually picked dispersion images used for the derivation of the shear wave velocity section on line 09SN_03BALST-M2. The dispersion curves (squares) are determined by linking the peaks of high energy. Note that 'higher modes' may at times produce higher energy peaks than the fundamental mode required for the analysis.
dotted fine line: signal-noise ratio for the designated f-v_{ph} – value.
red line: high resolution beam-forming curve for v_{max}.
1st row: left: station 70 @ PLUS direction; right: station 66 @ MINUS direction
2nd row: left: station 72 @ PLUS direction; right: station 68 @ MINUS direction
3rd row: left: not available due to bad quality; right: station 72 @ MINUS direction
4th row: left: not available due to bad quality; right: station 74 @ MINUS direction

3.3.4 Inversion of dispersion curves resulting in a 1D shear wave velocity distribution

Inversion of the extracted dispersion curves was performed using the algorithm described by Xia et al. (1999).

The inversion process is started by setting the maximum depth (z_{max}) to be in the order of 30% of the largest wavelength for an initial model consisting of 10 layers of increasing thicknesses. For all 10 layers the Poisson's ratio is assumed to be 0.4 and the rock/soil density to be 2.0 g/cm^3. The inversion process is concluded either after twelve iterations or when the convergence condition of a RMS-error of less than 3 m/s (phase velocity) is met.

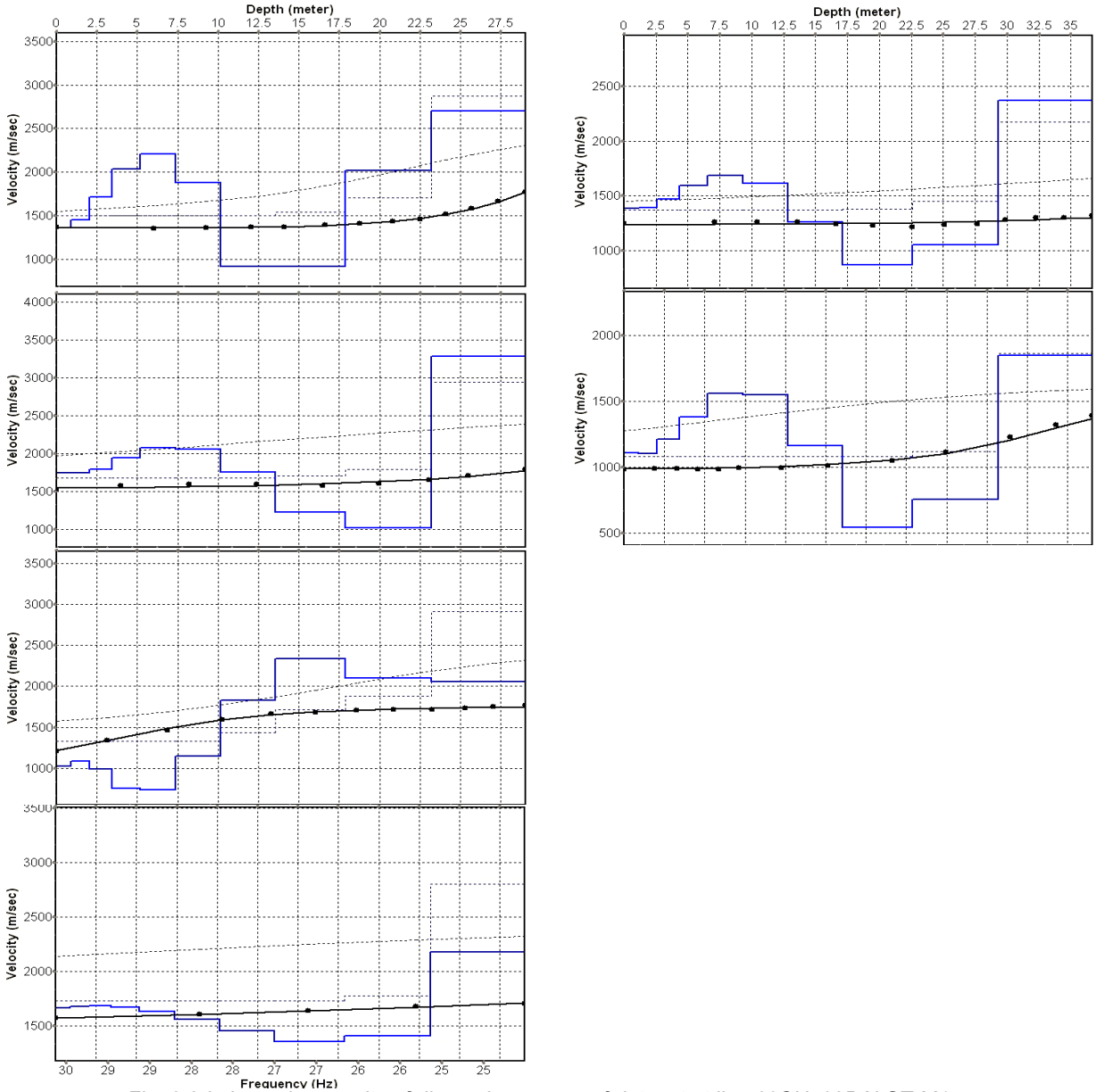

Fig. 3.3d: Inversion results of dispersion curves of dataset at line 09SN_03BALST-M1.
brown: Inversion of dispersion curve (dots) resp. of the modeled dispersion curve (dotted line: initial model; continuous line: end model). Horizontal axis: frequency Hz, vertical axis: vs.
blue: 10-layer-model (dotted: initial model, continuous line: final model). Horizontal axis: depth, vertical axis: phase velocity resp. v_s).
1st row: left: station 21 @ PLUS direction; right: station 24 @ MINUS direction
2nd row: left: station 33 @ PLUS direction; right: station 27 @ MINUS direction
3rd row: left: station 39 @ PLUS direction; right: not available
4th row: left: station 46 @ PLUS direction; right: not available
Due to bad quality dispersion plots in MINUS direction, only two inversions were computed in the representative section.

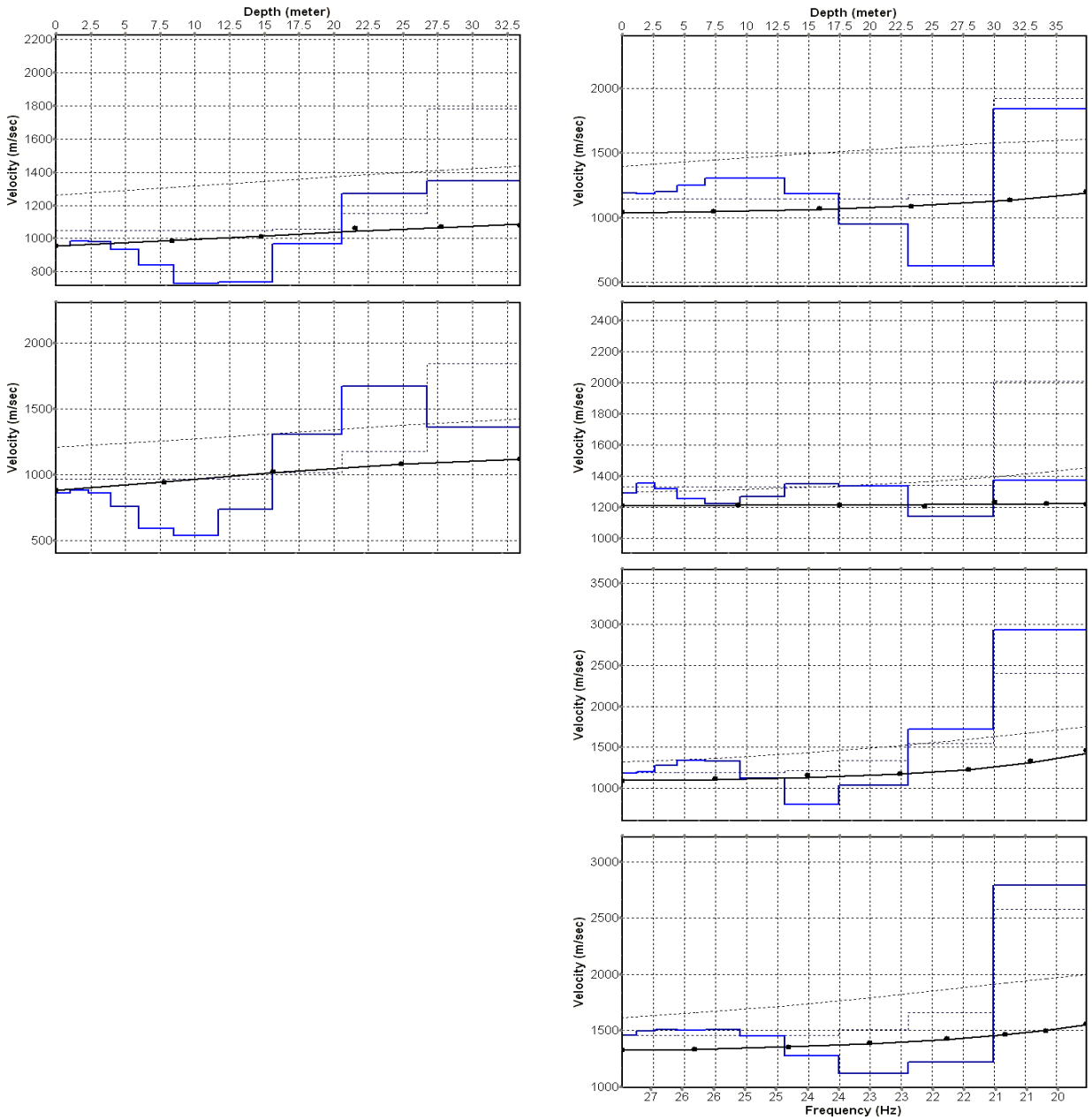

Fig. 3.3e: Inversion results of dispersion curves of dataset at line 09SN_03BALST-M2.
***brown**: Inversion of dispersion curve (dots) resp. of the modeled dispersion curve (dotted line: initial model; continuous line: end model). Horizontal axis: frequency Hz, vertical axis: v_s.*
***blue**: 10-layer-model (dotted: initial model, continuous line: final model). Horizontal axis: depth, vertical axis: phase velocity resp. v_S).*
1st row: left: station 70 @ PLUS direction; right: station 66 @ MINUS direction
2nd row: left: station 72 @ PLUS direction; right: station 68 @ MINUS direction
3rd row: left: not available right: station 72 @ MINUS direction
4th row: left: not available right: station 74 @ MINUS direction
Due to bad quality dispersion plots in PLUS direction, only inversions were computed in the representative section.

Dispersion analyses of records with longer receiver arrays should – by theory – increase the investigation depth. At BALST, with both lines and both directions, MASW processing with the maximal array length of 96 m doesn't improve the results (Fig. 3.3f and 3.3g).

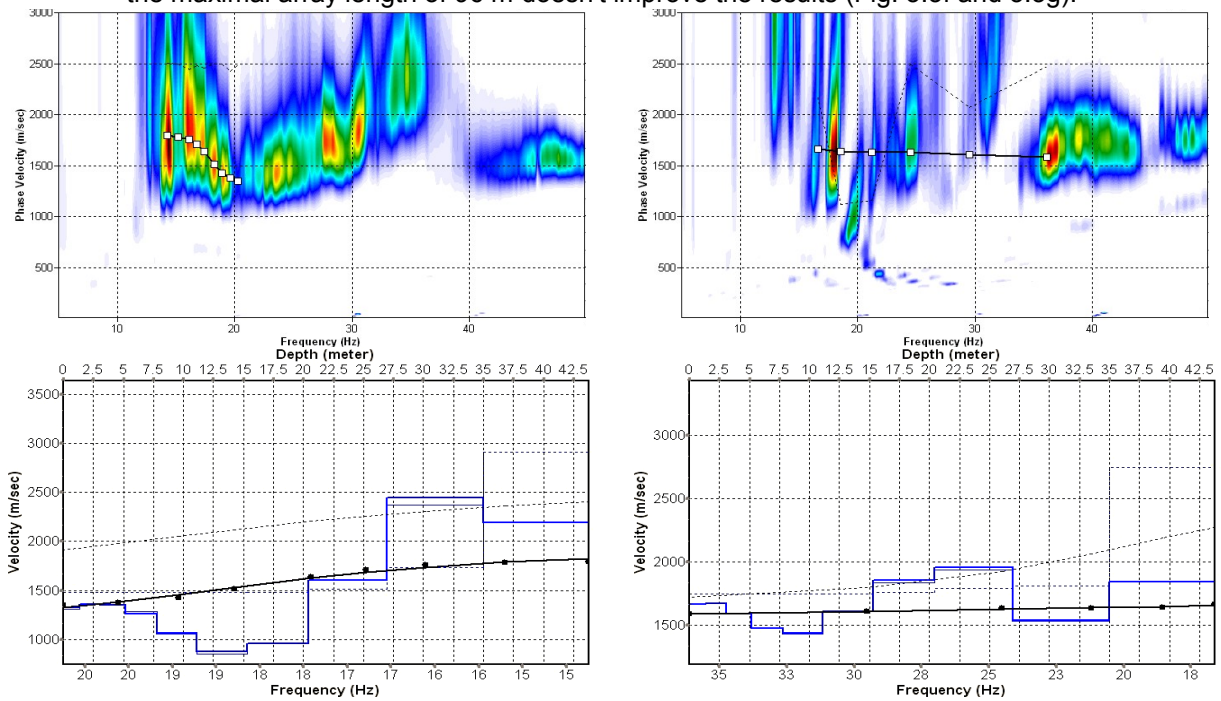

Fig. 3.3f: Top: dispersion images of over-all arrays (10...106 m offset) of line 09SN_03BALST-M1 in PLUS (left) and MINUS (right) direction; dotted fine line: signal-noise ratio for the designated f-v_{ph}-value.
*Below: The two respective inversion results; **brown**: inversion of dispersion curve; **blue**: 10-layer-model. Horizontal axis: depth, vertical axis: phase velocity resp. v_s.*

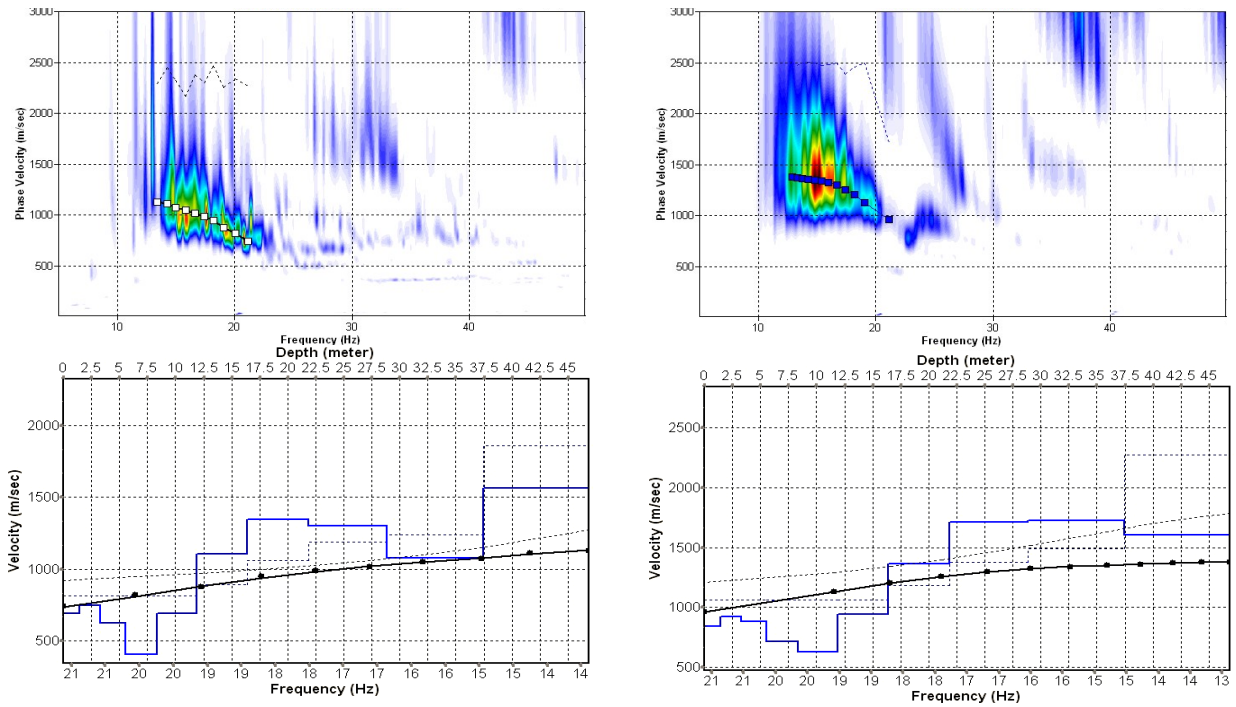

Fig. 3.3g: Top: dispersion images of over-all arrays (10...106 m offset) of line 09SN_03BALST-M2 in PLUS (left) and MINUS (right) direction; dotted fine line: signal-noise ratio for the designated f-v_{ph} – value.
*Below: The two respective inversion results; **brown**: inversion of dispersion curve; **blue**: 10-layer-model. Horizontal axis: depth, vertical axis: phase velocity resp. v_s.*

3.3.5 Gridding and plotting of 2D v_s-velocity field

By assembling the 1D v_s - depth functions of all stations the final 2D v_s-field is derived using a Kriging gridding procedure as portrayed in Fig. 3.3h and 3.3i below:

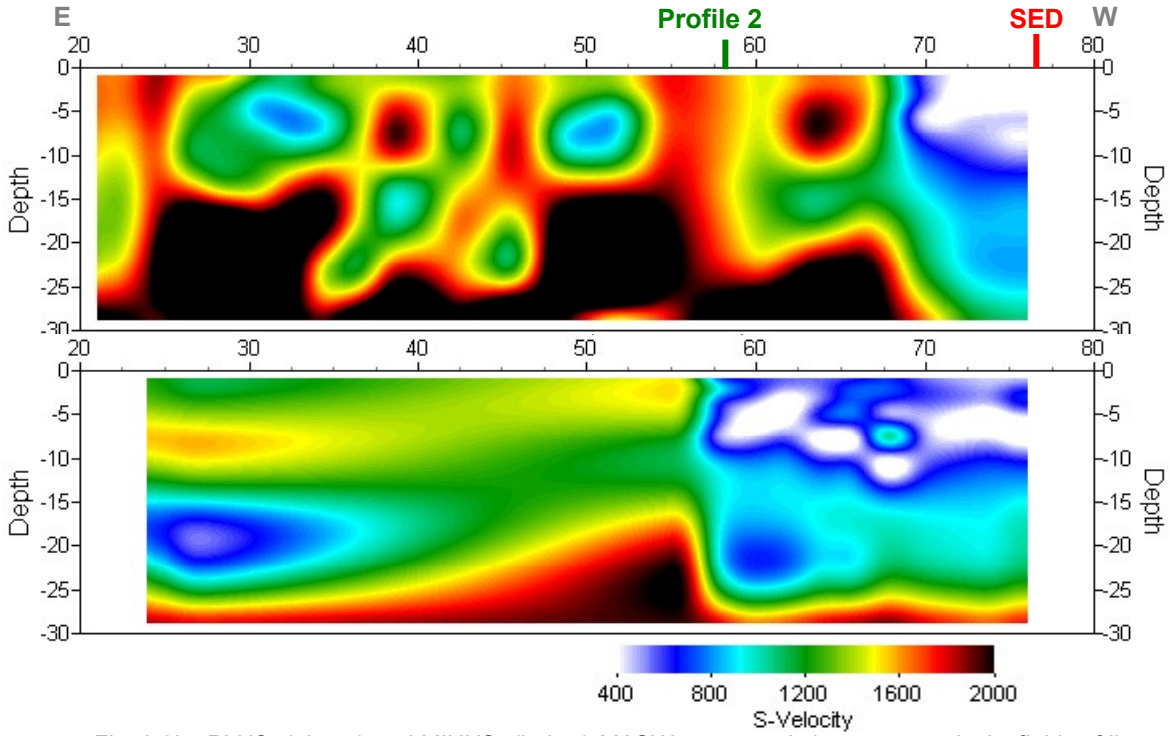

Fig. 3.3h: PLUS- (above) and MINUS- (below)-MASW-processed shear wave velocity fields of line 09SN_03BALST-M1. Station spacing is 1 m.

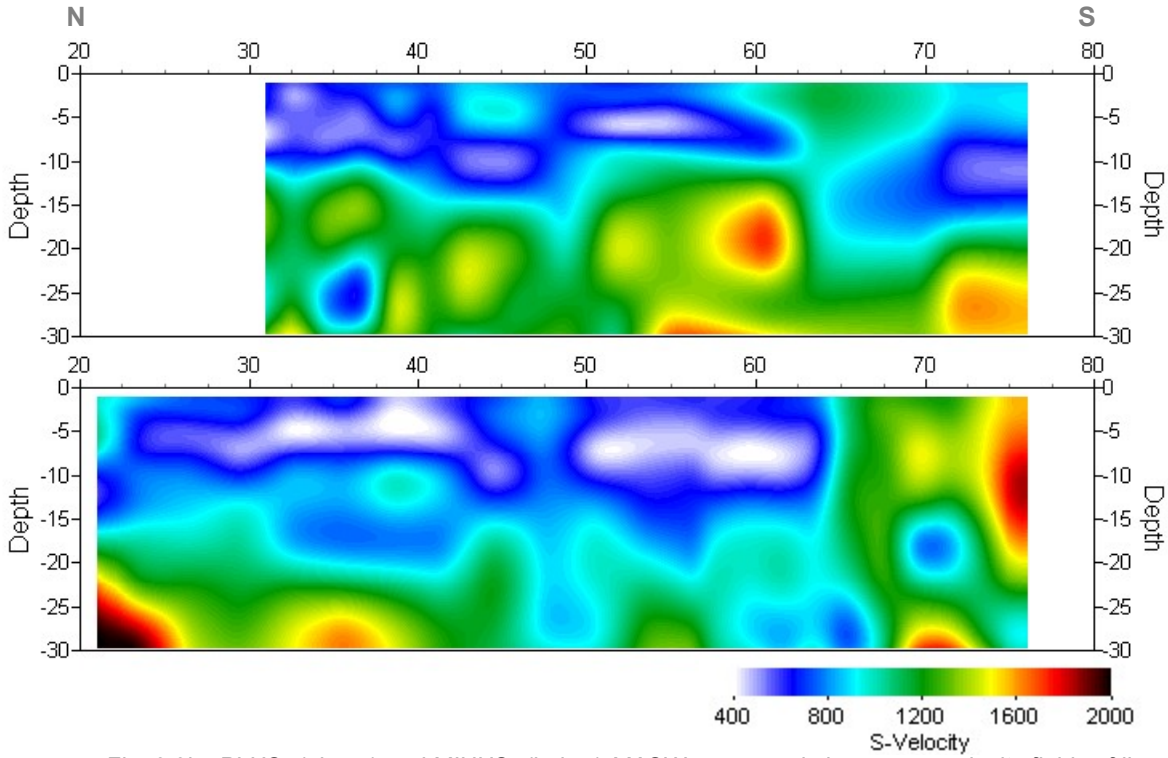

Fig. 3.3i: PLUS- (above) and MINUS- (below)-MASW-processed shear wave velocity fields of line 09SN_03BALST-M2. Station spacing is 1 m.

3.3.6 Calculation of the average shear wave velocity

In order to calculate a representative shear wave velocity-depth function of line 09SN_03BALST-M1 at the SED station, all computed 1D-v_s-depth functions between seismic profile station no. 20 and 50 are averaged (non-weighted mean values). On MINUS-direction, these are only two functions. The v_s-depth-function is shown in Tab. 3.3a.

Depth [m]	Vs- [m/s]	Vs+ [m/s]	Vs [m/s]
0.9	1184	1475	1330
2.0	1200	1464	1332
3.4	1263	1413	1338
5.2	1418	1333	1376
7.4	1555	1318	1436
10.1	1492	1384	1438
13.6	1114	1534	1324
17.9	650	1880	1265
23.2	981	2107	1544
29.0	1869	2247	2058

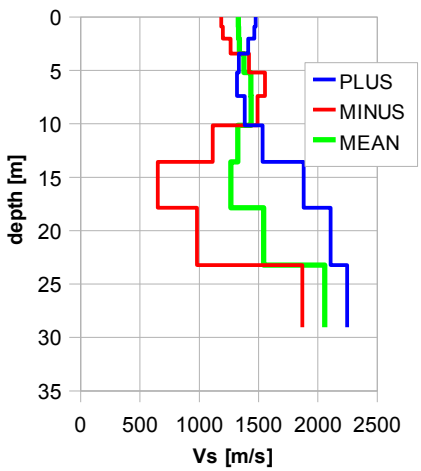

Tab. 3.3a: Averaged vs - depth function of line 09SN_03BALST-M1 at the SED station. Blue line: MASW-'PLUS' processing, red line: MASW-'MINUS' processing; green line: average of PLUS- and MINUS-functions.

In order to calculate a representative shear wave velocity-depth function of line 09SN_03BALST-M2 at the SED station, all computed 1D-v_s-depth functions between seismic profile station no. 65 and 75 are averaged (non-weighted mean values). The resulting v_s-depth-function is shown in Tab. 3.3b.

Depth [m]	Vs- [m/s]	Vs+ [m/s]	Vs [m/s]
1.1	1261	907	1084
2.5	1309	932	1121
4.2	1347	920	1133
6.3	1386	846	1116
9.0	1385	715	1050
12.4	1282	633	957
16.6	1048	738	893
21.8	1100	1135	1117
28.3	1315	1469	1392
35.4	2470	1354	1912

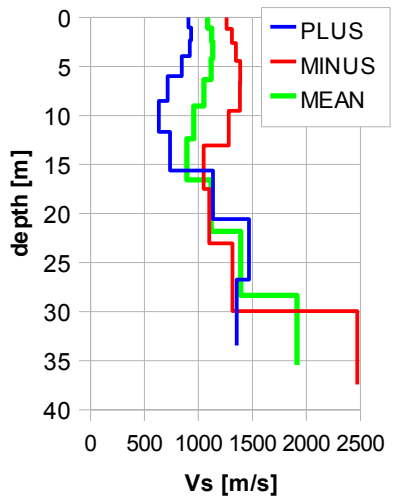

Tab. 3.3b: Averaged v_s - depth function of line 09SN_03BALST-M2 at the SED station. Blue line: MASW-'PLUS' processing, red line: MASW-'MINUS' processing; green line: average of PLUS- and MINUS-functions.

The inversion of the four 96 m-array dispersion curves data (20 to 116 m offset, see Fig. 3.3f and 3.3g) are given in Tab. 3.3c. These values are complemented with the values derived of the 40 m-arrays analyses (Tab. 3.3a and 3.3b).

100 m array								40 m array					
depth	m1+	m1-	m2+	m2-	m1	m2	m	depth	m1	depth	m2	depth	m
1.4	1329	1661	693	842	1495	767	1227	0.9	1330	1.1	1084	1.0	1207
3.2	1362	1669	745	919	1515	832	1259	2.0	1332	2.5	1121	2.2	1226
5.4	1351	1586	626	876	1468	751	1187	3.4	1338	4.2	1133	3.8	1236
8.1	1265	1473	407	709	1369	558	1048	5.2	1376	6.3	1116	5.8	1246
11.5	1061	1430	691	622	1246	657	1061	7.4	1436	9.0	1050	8.2	1243
15.8	879	1608	1107	938	1243	1023	1198	10.1	1438	12.4	957	11.3	1197
21.2	959	1852	1343	1359	1405	1351	1385	13.6	1324	16.6	893	15.1	1108
27.9	1606	1954	1301	1709	1780	1505	1621	17.9	1265	21.8	1117	19.8	1191
36.3	2443	1528	1076	1723	1985	1400	1682	23.2	1544	28.3	1392	25.8	1468
45.3	2188	1842	1562	1606	2015	1584	1864	29.0	2058	35.4	1912	32.2	1985

Tab. 3.3c: v_s-depth values of the four MASW-derived dispersion curves of both seismic line 09SN_03BALST-M1 and 09SN_03BALST-M2 using 100 m-arrays. The dispersion curves are shown in Fig. 3.3f and Fig 3.3g.

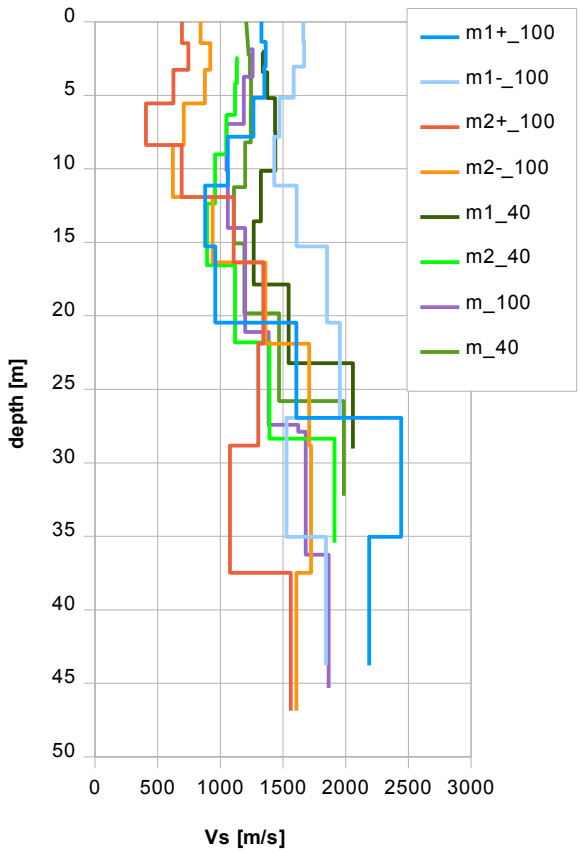

Fig. 3.3j: Comparison of the ensemble of inversion results of both lines 09SN_03BALST-M1 and -M2, either using the 40 m- and the 100 m-arrays.
blue lines: analyses of records of line 09SN_03BALST-M1
red lines: analyses of records of line 09SN_03BALST-M2
magenta line: mean of both 100 m-array records analyses in MINUS and PLUS direction.
green lines: v_s-values of analyses of 40 m-array records.

3.3.7 Calculation of the shear wave velocity scalars $v_{s,5}$, $v_{s,10}$, ...

The parameters $v_{s,5}$, $v_{s,10}$, $v_{s,20}$, $v_{s,30}$, $v_{s,40}$, $v_{s,50}$ represent the average shear wave velocities in the depth interval between the surface and the respective depth levels and are determined from the formula

$$v_{s,n} = \frac{\sum_{i=1}^{n} d_i}{\sum_{i=1}^{n} d_i / v_{si}}$$

with:

d_i = thickness of layer i

v_{si} = corresponding shear-wave velocity.

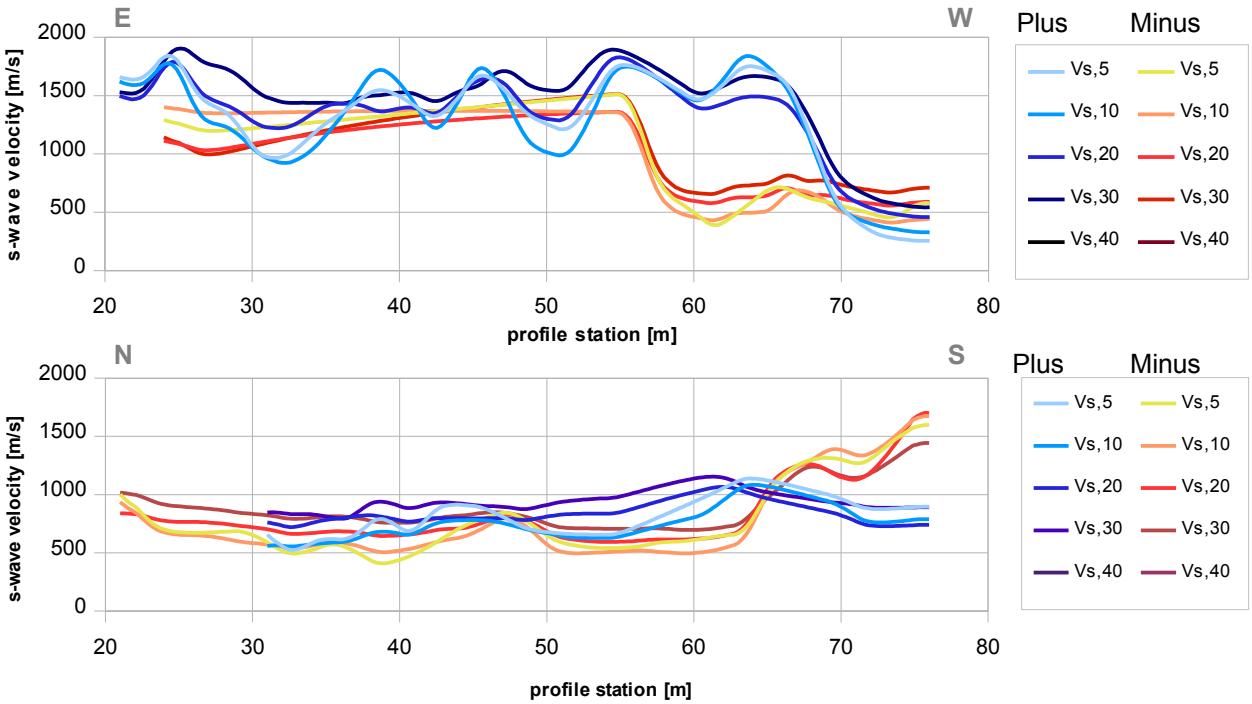

Fig. 3.3k: Graphs of the averaged $v_{s,5}$...-values along the line 09SN_03BALST-M2 for the PLUS- (blue lines) and MINUS- (red lines) directions.

The average values of the s-wave velocity model $v_{s,5}$, $v_{s,10}$, $v_{s,20}$, $v_{s,30}$, $v_{s,40}$, $v_{s,50}$, $v_{s,100}$ (= average shear wave velocity from the surface to depths of 5 m, …until 100 m) on the line segment nearest to the SED station (Tab. 3.3d) are summarized below:

	Vs,5	Vs,10	Vs,20	Vs,30	Vs,40	Vs,50
MINUS	1317	1365	1203	1244	n/a	n/a
PLUS	1411	1358	1440	1578	n/a	n/a
MEAN	1364	1362	1321	1411	n/a	n/a

	Vs,5	Vs,10	Vs,20	Vs,30	Vs,40	Vs,50
MINUS	1335	1374	1291	1222	n/a	n/a
PLUS	965	883	816	930	n/a	n/a
MEAN	1150	1129	1053	1076	n/a	n/a

Tab. 3.3d: The average shear wave velocities within the depth intervals from surface down to 5 m, etc.… to 50 m, calculated for the line segment with a subjectively most similar geology to the SED station (profile station 20 to 50 for line 09SN_03BALST-M1, top; profile stations 65 to 75 for line 09SN_03BALST-M2, bottom).

3.4 Hybrid Seismic Data Processing

3.4.1 p-wave *Reflection* Seismic Processing Sequence

A) Data conditioning

A1 Reformatting and quality verification of field data
A2 Recording geometry assignment
A3 Data editing (suppression of bad / dead traces, etc.)
A4 Preliminary analysis of refraction velocities

B Filtering and deconvolution

B1 Analytical muting of refraction arrivals
B2 Amplitude recovery / amplitude equalization in time and frequency domains
B3 Predictive deconvolution parameter tests / application
B4 Determination of band limiting corner frequencies / application
B5 Optional 2-D filtering

C) Velocity analysis and stack

C1 Common Depth Point (CDP) sort
C2 Semblance velocity analysis using supergathers of 3 - 5 CDP's
C3 Optional dip move-out correction
C4 Normal Move-Out (NMO) correction and application of stretch mute
C5 Band-pass filtering
C6 CDP stack
C7 Optional coherency filtering

D) Time-depth conversion

D1 Optional spiking deconvolution
D2 Band-pass filtering
D3 Depth conversion
D4 Final display of seismic depth section with inversed polarity (non-SEG-convention)

3.4.2 The presentation of reflection seismic data

The data in a reflection seismic section are presented as an assembly of individual seismic signals at regular intervals along a seismic profile. The simplest way of representing the signals are single wiggle lines (first to the left in the illustration below). A more capturing presentation is the variable area form (second to the left). Combining these two modes results in the var-wiggle mode. Another method of data visualization is the variable density mode (second from the right).

The compressional phase of seismic signals is defined in this report as the onset of the positive amplitude excursion in black (Fig. 3.4a). Since the source signal is produced by an explosion or by an impact at the surface, the signal starts off with a compression of the ground particles. Thus the arrivals of reflection events are defined by the compressional phase.

In rare situations of velocity inversions, cases in which formation velocities are lower than in the layers above, polarity reversals of the reflected signals occur. The beginning of the reflection event would then be characterized by a dilatational phase, represented in this report as a negative amplitude excursion, i.e. in white.

The final p-wave seismic depth sections are displayed in Fig. 3.4b and 3.4c, the hybrid sections in Fig. 3.4j and -k further below.

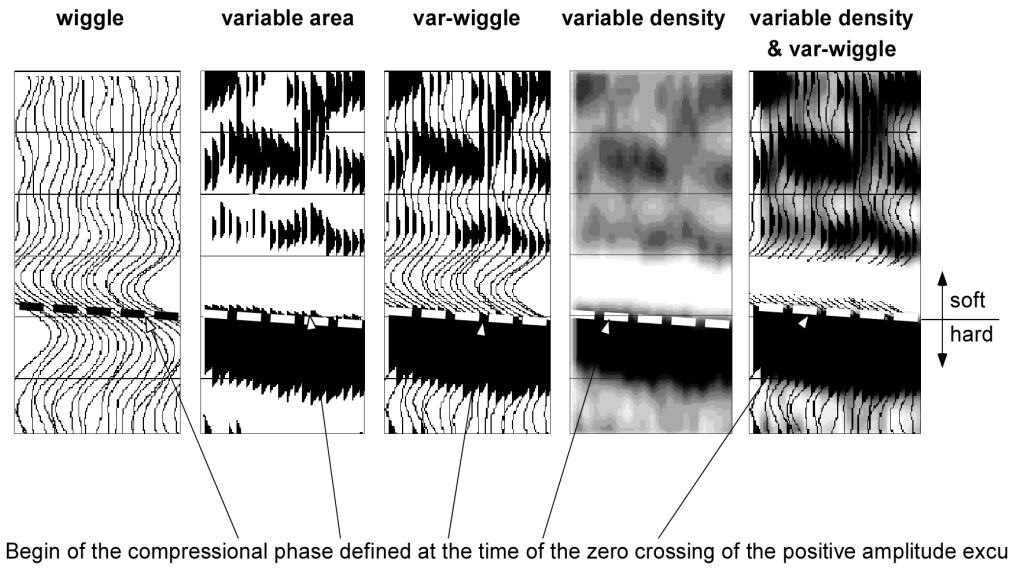

Fig. 3.4a Representation of reflection seismic data and the definition of a reflection event.

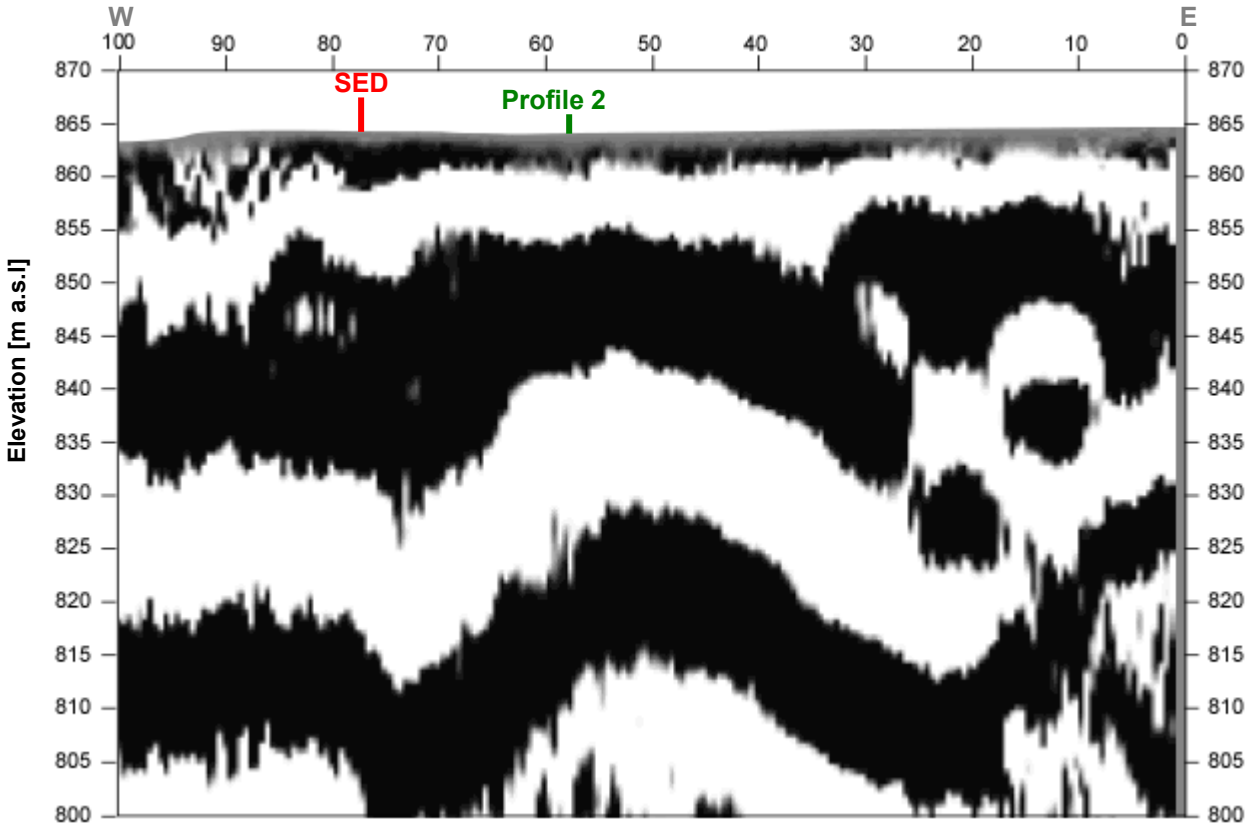

Fig. 3.4b: Seismic depth section of seismic line 09SN_03BALST-P1 with variable density mode presentation. Vertical axis: elevation [m a.s.l.], horizontal axis: profile meter; no vertical exaggeration. The station spacing is 1 m.

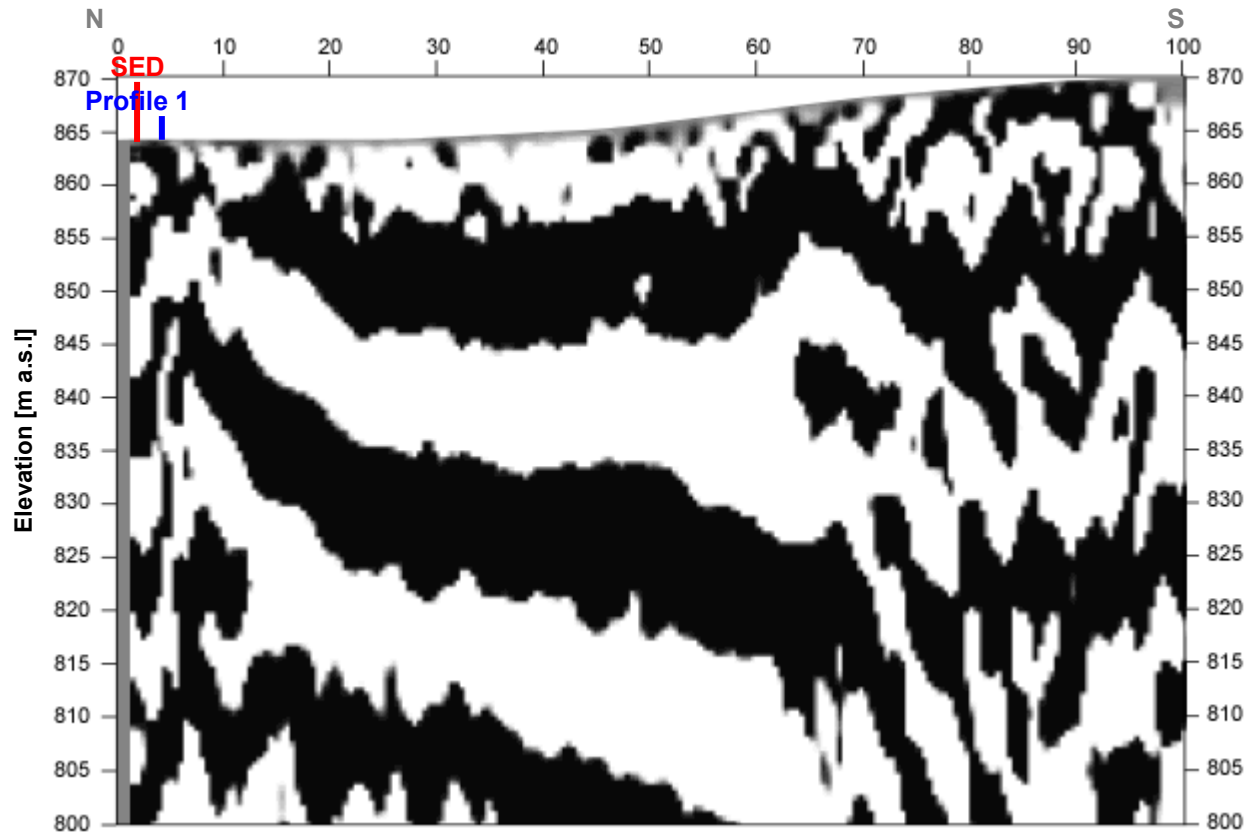

Fig. 3.4c: Seismic depth section of seismic line 09SN_03BALST-P1 with variable density mode presentation. Vertical axis: elevation [m a.s.l.], horizontal axis: profile meter; no vertical exaggeration. The station spacing is 1 m.

3.4.3 p-wave refraction tomography processing

The seismic p-wave refraction processing steps are analogous to those described in paragraph 3.2. For a detailed method statement and a description of the processing steps please refer to the summary report. The Figs. 3.4d to 3.4i and Tab. 3.4a illustrate the intermediate processing steps and the final result.

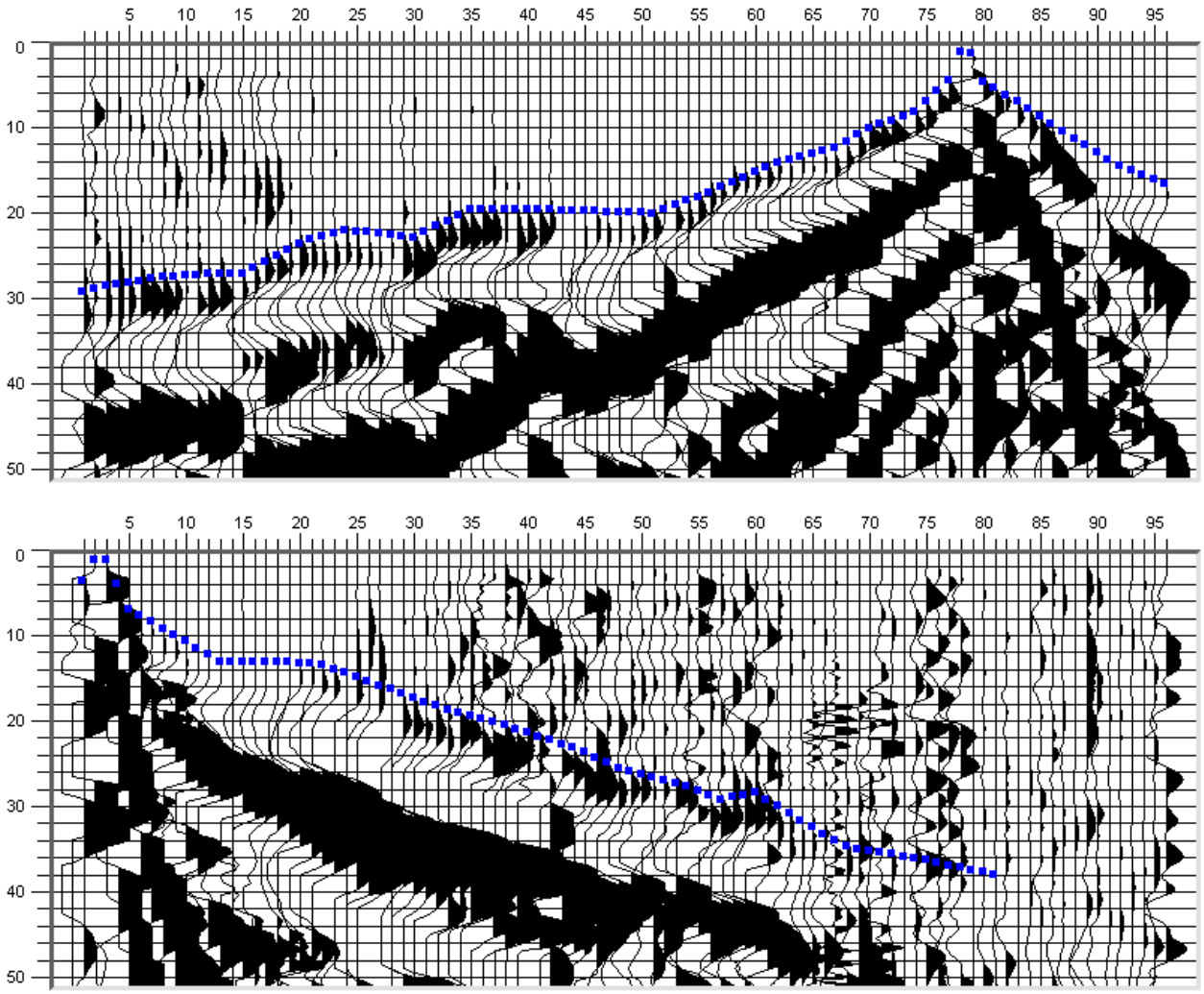

Fig. 3.4d: p-wave records of 09SN_03BALST-P1 (above) and -P2 (below) with positive amplitude excursions in black. Blue squares mark the manually picked first break arrival times. Vertical axis: travel time in ms, horizontal axis: station numbers spaced at 1 m.

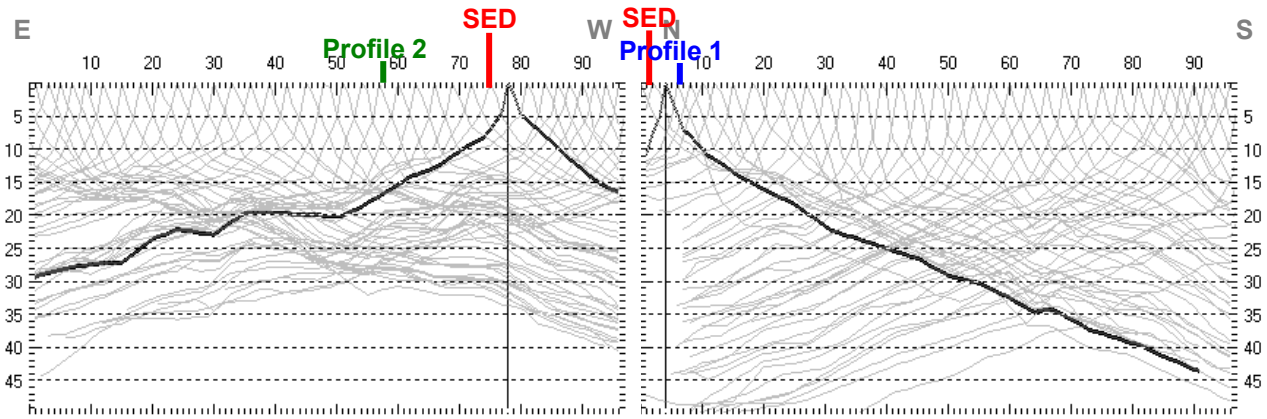

Fig. 3.4e: Travel time curves of p-wave arrival time picks of line 09SN_03BALST-P1 (left) and -P2 (right). Vertical axes: travel time [ms], horizontal axes: station number (= profile meter).

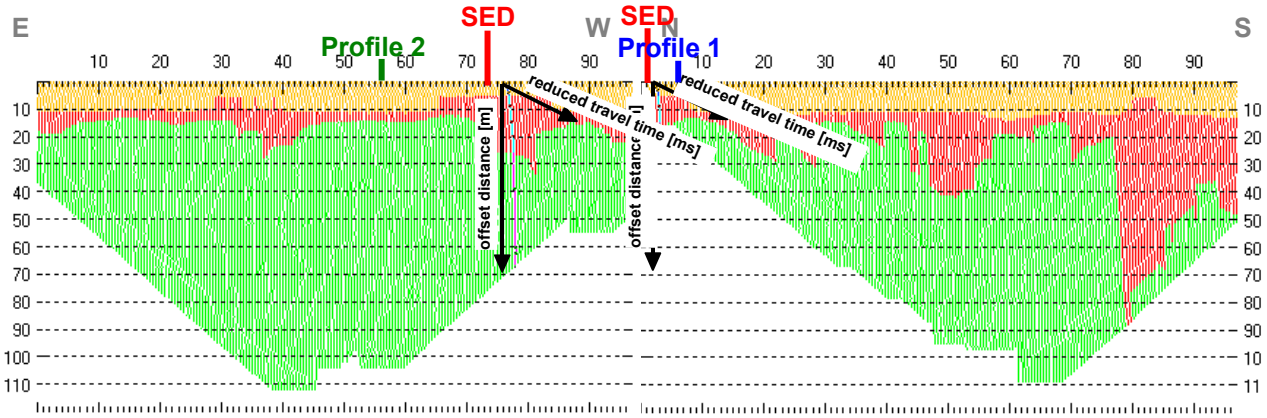

Fig. 3.4f: 3-dimensional distance-travel time diagrams at the mid-points between source points and receiver stations are instrumental when using the analytical CMP derivation of the initial velocity field. The horizontal axes are along the CMP positions and the travel time respectively, the vertical axis denotes the offset distance between source and receiver positions.

Depth [m]	Vp [m/s]
0.0	342
0.2	365
0.5	449
1.2	646
1.7	841
2.5	1217
3.5	1635
4.7	2160
6.5	3081
8.7	3837
11.7	3973
15.5	4126
20.5	4371
27.2	4538
36.0	5074

Depth [m]	Vp [m/s]
0.0	289
0.2	331
0.5	437
0.9	512
1.4	651
1.9	800
2.7	1022
3.8	1416
5.3	1907
7.0	2140
9.6	2226
12.6	2382
16.7	2314
22.2	2543
29.2	2940

Tab. 3.4a: Initial 1D p-wave velocity model derived from real data (left: 09SN_03BALST-P1; right: -P2).

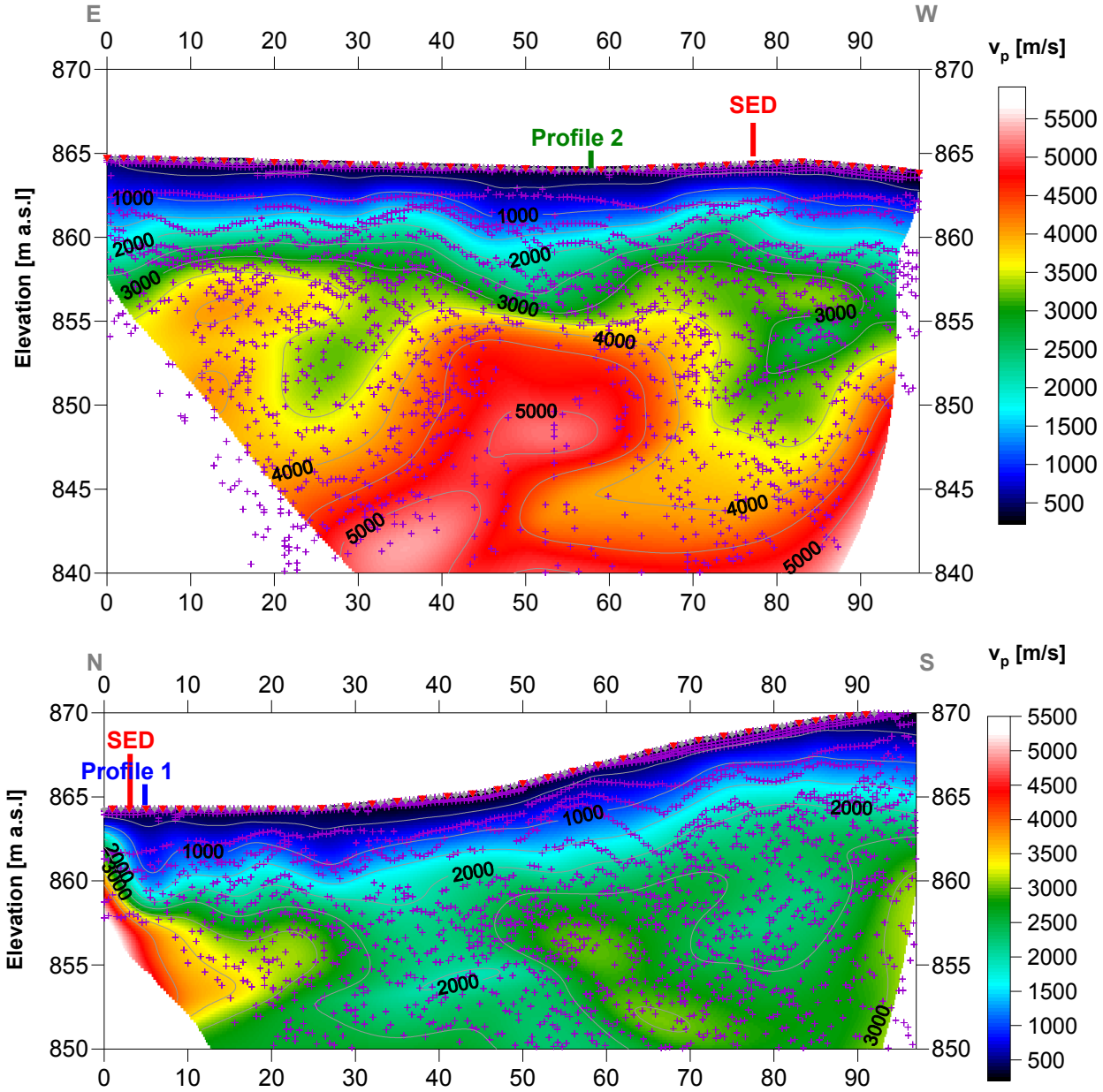

Fig. 3.4g: Compressional wave velocity field image along the seismic profiles 09SN-03BALST-P1 (above) and -P2 (below). Red/white colors indicate solid rock, blue/black colors unconsolidated sediments and soil. Vertical axis: elevation [m a.s.l]; horizontal axis: profile meter; color scale: vs [m/s]; vertical exaggeration: 2:1; gray squares: receiver stations; red triangles: shot positions; magenta crosses: positions of determined velocity values.

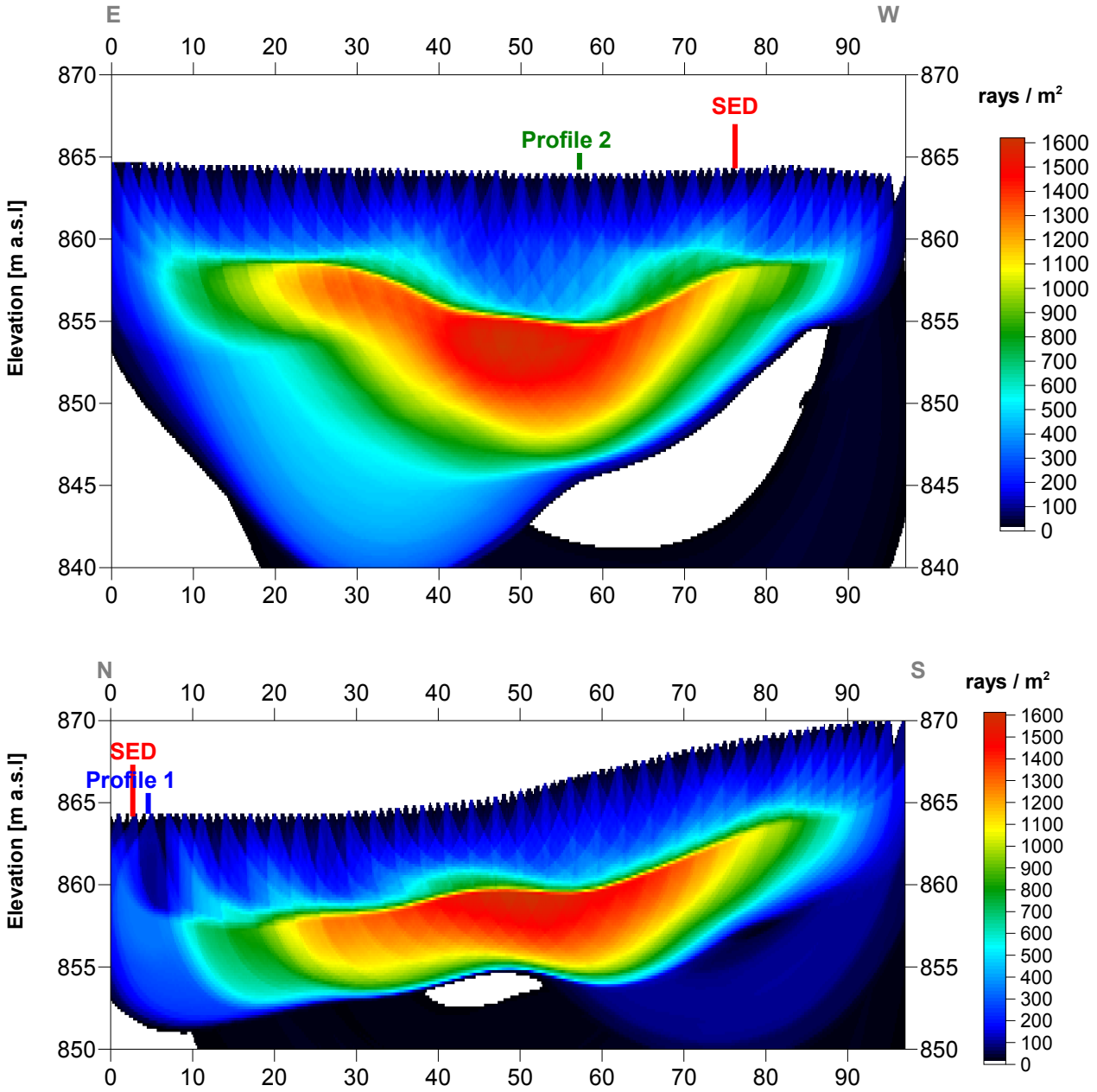

Fig. 3.4h Compressional wave subsurface ray path density along the seismic profiles 09SN_03BALST-P1 (above) and -P2 (below). Red/white colors indicate high velocity contrast between two layers, blue/black colors low coverage areas. Vertical axis: elevation [m a.s.l]; horizontal axis: profile meter; color scale: ray paths per m2; vertical exaggeration: 2:1.

Depth [m]	Vp [m/s]
0.0	348
1.8	862
3.5	1589
5.2	2417
6.8	3053
8.5	3473
10.2	3885
11.8	4065
13.5	4180
15.2	4334
16.8	4444
18.5	4458
20.2	4593
21.9	4813
23.5	5019
25.2	5134
26.9	5347
28.5	5537
30.2	5687
31.9	5825

Depth [m]	Vp [m/s]
0.0	310
1.9	852
3.8	1460
5.6	2052
7.5	2428
9.4	2547
11.3	2564
13.1	2643
15.0	2773
16.9	2814
18.8	2706
20.6	2632
22.5	2674
24.4	2773
26.3	2900
28.1	3051
30.0	3217
31.9	3395
33.8	3605
35.7	3854

Tab. 3.4b: Final 1D p-wave velocity model derived from real data at positions most similar to the geological setting at SED station between profile meters 20 and 50 at line 09SN_03BALST-P1 (left) resp. 65 and 75 at line 09SN_03BALST-P2 (right) .

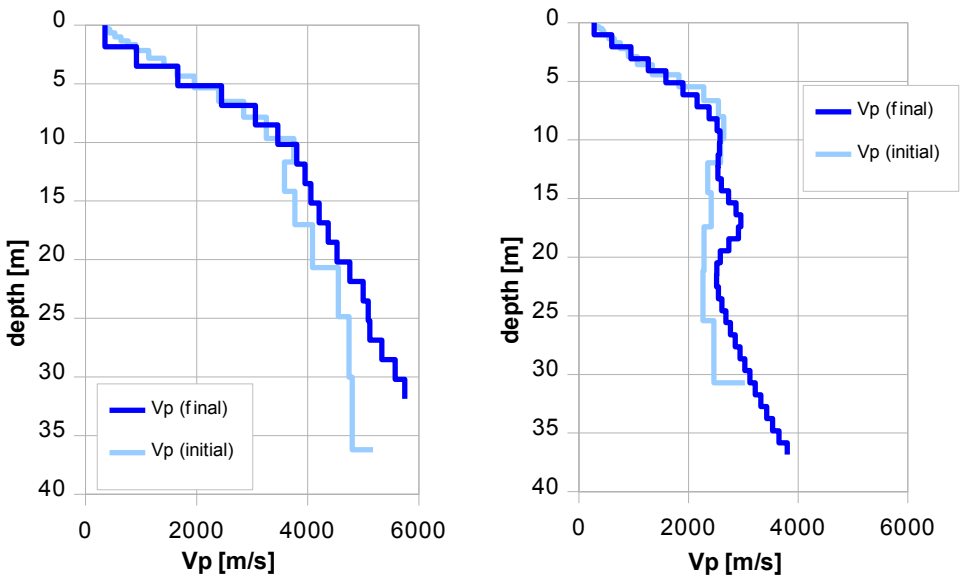

Fig. 3.4i: Final 1D p-wave velocity model derived from real data at a position most similar to the geological setting at the SED station between profile meters 20 and 50 at line 09SN_03BALST-P1 (left) resp. 65 and 75 at line 09SN_03BALST-P2 (right). Initial 1D p-wave velocity model values are given in Tab. 3.4a.

3.4.4 Representation of the hybrid seismic section

The hybrid seismic section is the reflection seismic section with the superimposed p-wave velocity field. It portrays the geological structures and the p-wave velocity field, the latter being indicative for the rock / soil rigidity. The uninterpreted hybrid seismic section is portrayed in Fig. 3.4j and 3.4k on next page.

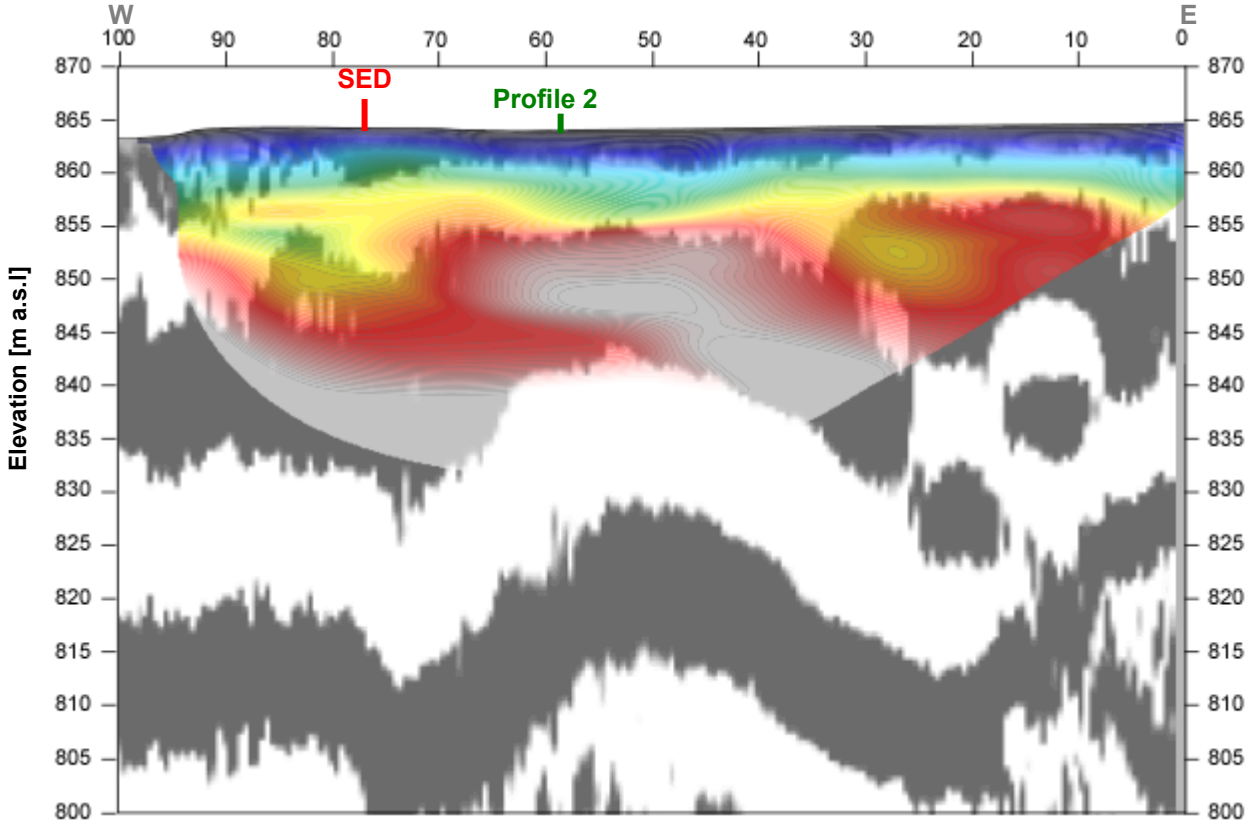

Fig. 3.4j Uninterpreted hybrid seismic section 09SN_03BALST-P1: superimposed onto the seismic reflection section is the color encoded p-velocity field derived by refraction tomography (no vertical exaggeration).

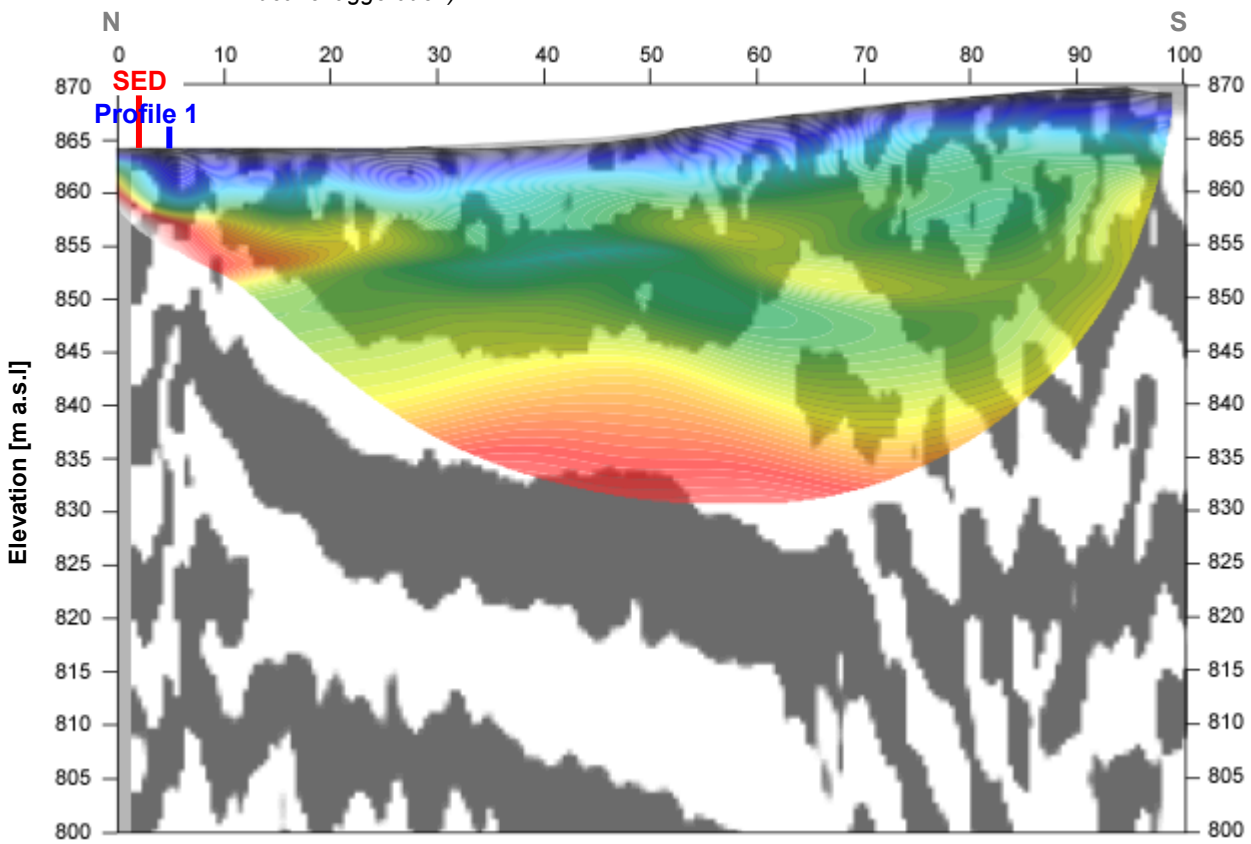

Fig. 3.4k Uninterpreted hybrid seismic section 09SN_03BALST-P2: superimposed onto the seismic reflection section is the color encoded p-velocity field derived by refraction tomography (no vertical exaggeration).

4 DISCUSSION OF THE RESULTS

4.1 Summary and Validation of the Results

Compressional and shear wave velocity data from refraction seismic surveys both p-wave and s-wave and also the MASW survey data of profiles 09SN_03BALST-1 and 09SN_03BALST-2 are shown in Tab. 4.1 for the uppermost 30 m. The calculated shear wave velocity $v_{s(calc)}$ in Tab. 4.1 is derived by using a theoretical v_p/v_s-ratio of $\sqrt{3}$.

Depth	Vp1	Vp2	Vs1	Vs2	Vs1	Vs2	Vs1	Vs2
	meas	meas	meas	calc	meas	calc	MASW	MASW
0	353	276	155	204	155	159	1330	1084
1			345		322			
2	353	601	662	204	553	347	1332	1121
3		952	955		694	550	1338	1121
4	919	1268	1218	530	918	732		1133
5	1661	1589	1345	959	1128	917	1376	
6		1900	1302		1428	1097		1116
7	2449	2159	1249	1414	1598	1246	1436	
8		2374	1243		1471	1370		
9	3059	2523	1275	1766	1135	1457		1050
10	3462	2575	1330	1999	859	1487	1438	
11		2564	1393		739	1480		
12	3802	2538	1468	2195	670	1465		957
13		2536	1575		669	1464		
14	3953	2598	1685	2282	684	1500	1324	
15	4054	2732	1769	2341	708	1577		
16		2865	1799		733	1654		
17	4204	2953	1835	2427	777	1705		893
18		2911	1850		818	1681	1265	
19	4366	2737	1876	2520	895	1580		
20	4525	2577	1943	2613	928	1488		
21		2515	2025		957	1452		
22	4757			2747	983			1117
23		2512			1006	1450	1544	
24	4996	2546		2884	1027	1470		
25	5087	2606		2937	1049	1505		
26		2682			1101	1548		
27	5118	2764		2955	1137	1596		
28		2850			1196	1645		1392
29	5334	2937		3080	1276	1696	2058	
30	5570	3027		3216	1339	1748		

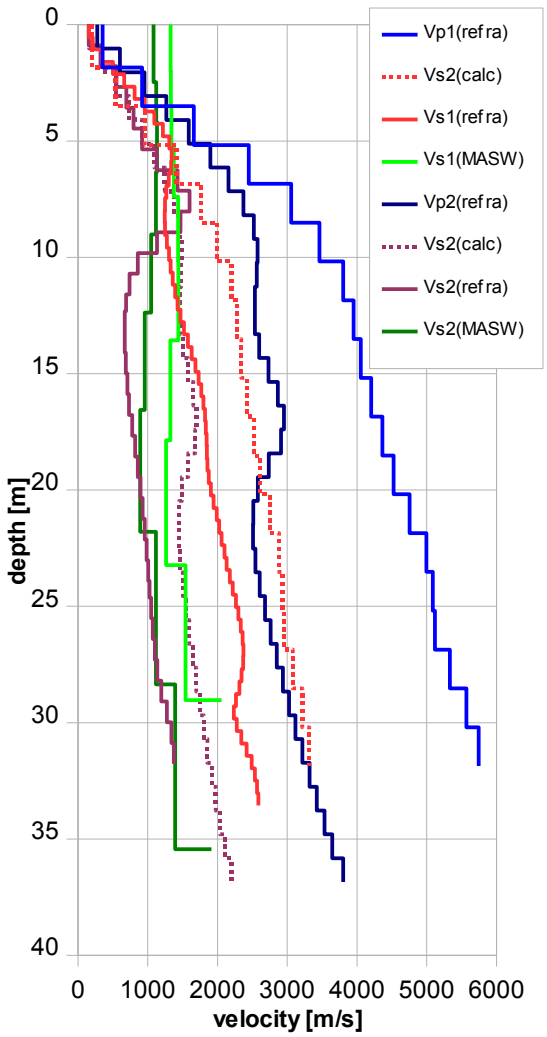

Tab. 4.1: Shear and compressional wave velocity model determined at the SED station.

Fig. 4.1: Graphic display of shear (red) and compressional (blue) wave refraction tomography velocities determined at the SED station. In green colors values of MASW analyses. The dotted lines gives the theoretical maximum shear wave velocity derived from compressional wave velocities..

4.2 Validation of the methods and their results

The geological setting at BALST shows various heterogeneities due to karstified rock (sinkholes). These heterogeneities can be imaged better by refraction tomography than by surface waves analyses because the seismic field of surface waves is highly deranged. So the velocities may differ significantly between the two shear wave velocity derivation methods.

4.3 Error Estimates

The error estimates given in Tab. 4.3 below are relevant only in the context of this survey.

Surveying method	Type of result	Error estimate
v_s – refraction tomography	v_s – velocity field image	15%
MASW only "+" or only "-" values*	v_s – velocity field image	20%
MASW (mean of "+" & "-" values)*	v_s – velocity field image	15%
v_p – refraction tomography	v_p – velocity field image	10%
Reflection seismic surveying	Image of subsurface structures	n.a.

** MASW values in the uppermost 5 m are prone to an error of about 50 %. The values does not express shear wave velocities of soil and weathered rock.*

Tab. 4.3 Error estimates for the methods applied. Note that higher error estimates are to be taken into account with increasing depths.

The above error estimates are of a qualitative character only. In view of the intense fluctuations due to karstified rock to be expected in both the lateral and vertical directions, any attempt to derive a quantitative general error estimate to be valid for the entire survey is to be considered as futile. In particular on line 09SN_03BALST-M1, the values of MINUS direction of seems to be too low, with an error of more than 50%. This high error is caused by bad quality dispersion image and few inversions running with reliable results.

At the SED station BALST (Mümliswil SO), the refraction velocity images both from shear and compressional wave analysis show in outlines coincident structures. The MASW figures of hardrock (below depth of 5 m) are in the same range as the values obtained from the shear wave diving wave refraction tomography surveys.

4.4 The Geophysical Interpretation

The most conclusive information about the subsurface structures is provided by the results of the hybrid seismic section (v_p-refraction tomography profiling and reflection seismic section) and confirmed by the evaluation results of the v_s-refraction tomography data.

As can be seen from the v_s and v_p refraction tomography sections in Fig. 3.2e/f & Fig. 3.4g/h, the topography of the bedrock surface is imaged in detail on both profiles. The geological interpretation of the seismic events is shown in Fig. 4.2a. The bedrock surface seems to be in a depth between 3 and 8 meters, smoothly undulating along the line. Two areas with reduced velocities may correspond with locally prevalent karst phenomena stringed to supposed tectonic faults.

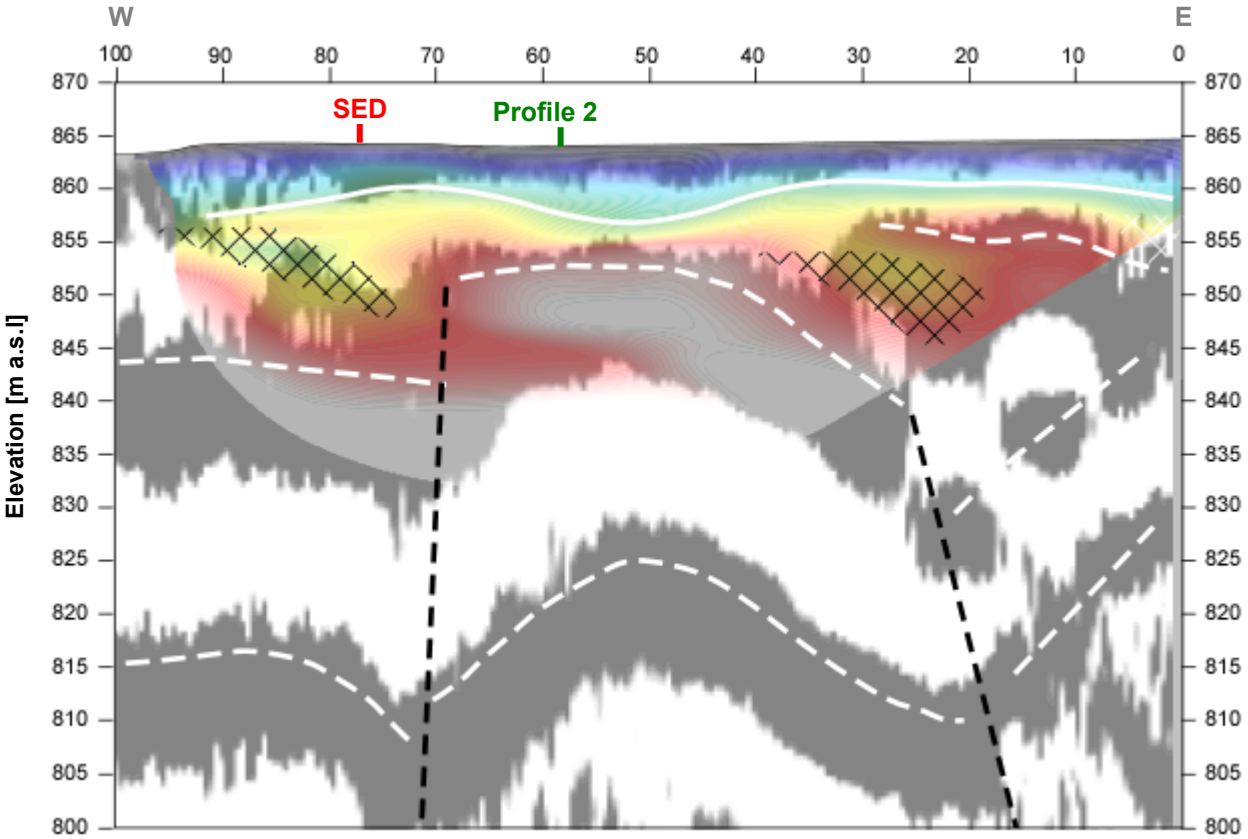

Fig. 4.2a Geophysical interpretation of the hybrid seismic section 09SN_03BALST-P1. White lines denote layer boundaries, continuous line the bedrock surface. Suspected tectonic faults are marked with black dashed lines and proposed karstified bedrock is outlined with black hatched areas.

The geological interpretation of the seismic events of line 09SN_03BALST-2 is shown in Fig. 4.2a. The bedrock surface seems to be in a depth of about 2 to 6 m below terrain. To the North of the profile, the bedrock outcrops to the steep cliff obviously visible in the field. An even settled layering in bedrock changes abruptly to a remarkably heavy karstified zone in the South of the section. It correspond extraordinarily well with the sinkholes visible in field and mapped at www.sogis.ch.

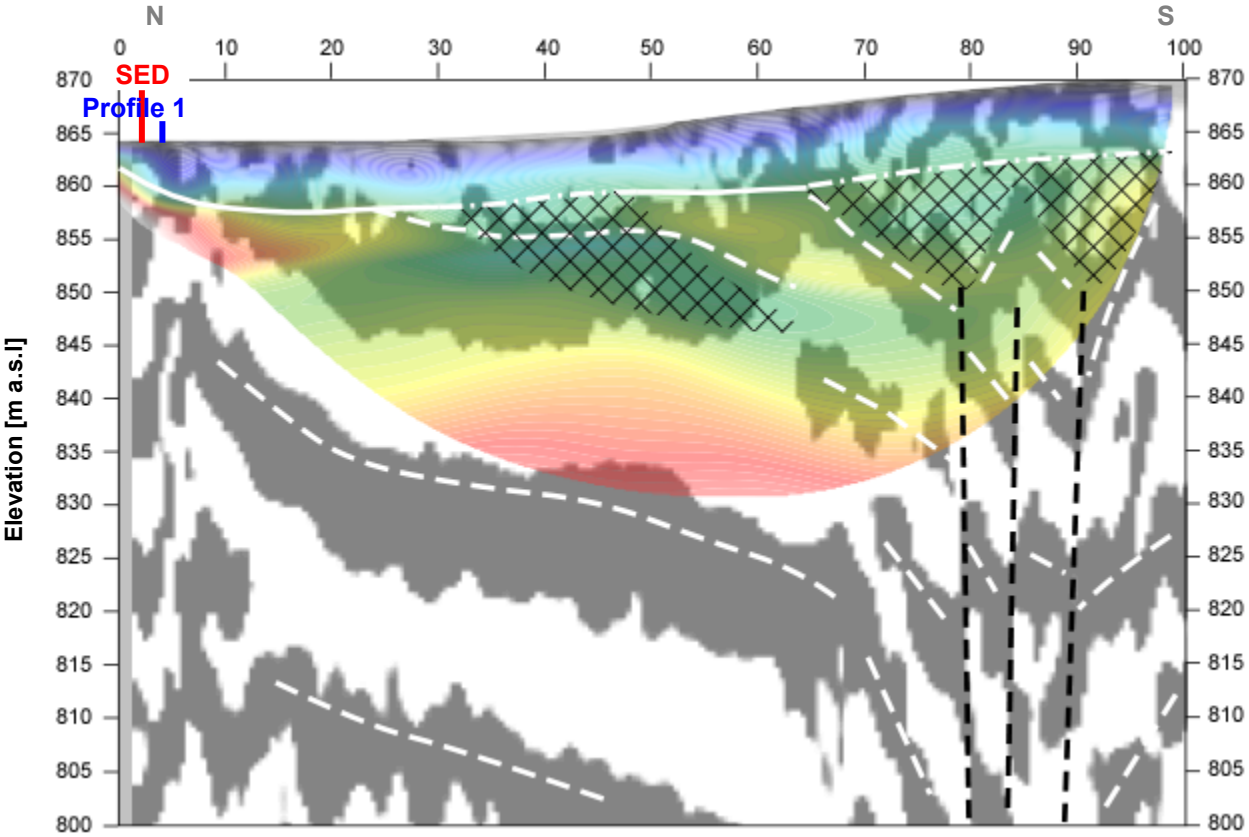

Fig. 4.2b Geophysical interpretation of the hybrid seismic section 09SN_03BALST-P2. White lines denote layer boundaries, the continuous one marks the bedrock surface; black dotted lines are indicative of suspected faulting with a wide karstified zone (black hatched area).

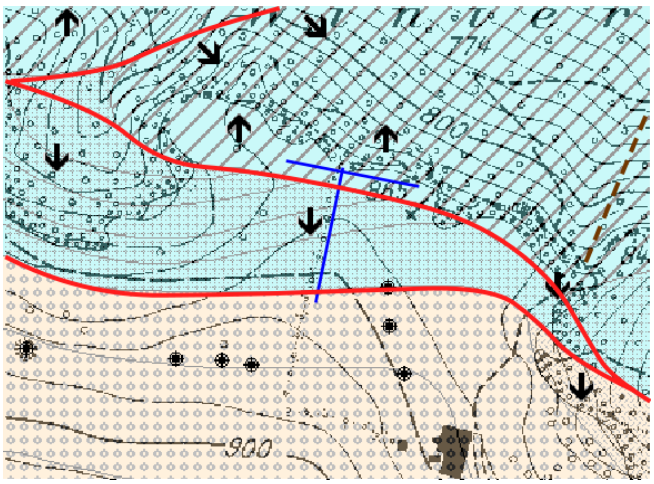

Fig. 4.2c Detail from geological map (source: www.sogis.ch) with marked sinkholes (black dots) and dipping of the layering (arrows). Colors denotes lithological units (yellow: Dogger, blue: Malm), red and brown lines tectonic lineaments. The two seismic traces are given in blue.

5 SUMMARY AND CONCLUSIONS

- In May 2009 a combined seismic s- and p-wave survey was carried out at the SED earthquake monitoring station BALST near Mümliswil SO.
- The shear wave data have been evaluated by conventional diving wave refraction tomography techniques in order to derive the s-wave velocity field along the seismic line.
- The p-wave data have been processed
  - firstly to derive a 2D s-wave velocity field by using the MASW (**M**ultichannel **A**nalysis of **S**urface **W**aves) technique;
  - and secondly, according to the hybrid seismic data processing scheme for representing the subsurface structures in a combined reflection seismic section with the superimposed p-wave velocity field.
- The shear wave velocity range determined by the MASW method in the uppermost 30 meters spans from values of 893 m/s to 1544 m/s.
- The scalar values derived by the MASW survey at the SED station are the following:

line 1			line 2		
$v_{s,5}$	=	1364 m/s	$v_{s,5}$	=	1150 m/s
$v_{s,10}$	=	1362 m/s	$v_{s,10}$	=	1129 m/s
$v_{s,20}$	=	1321 m/s	$v_{s,20}$	=	1053 m/s
$v_{s,30}$	=	1411 m/s	$v_{s,30}$	=	1076 m/s
$v_{s,40}$	=	n/a	$v_{s,40}$	=	n/a

- The reliable bedrock refraction shear wave velocity derived is around 1600 m/s.
- The reliable bedrock p-wave velocity determined is around 4000 m/s.
- The two seismic profiles show significantly differing velocities. Line 2 seems to reflect generally loosened bedrock (supposed as karstified limestone).
- The geophysical interpretation of the subsurface structures in this report are to be validated and incorporated into a comprehensive appraisal by a geologist familiar with the local geological setting.

Schwerzenbach, 7th July 2009

Walter Frei
dipl. Natw. ETH
managing director

Lorenz Keller
dipl. Natw. ETH
project manager